LUND UNIVERSITY

One-dimensional pulse propagation in temporally dispersive media - exact solutions versus numerical results

Rikte, Sten

1997

Link to publication

Citation for published version (APA):
Rikte, S. (1997). *One-dimensional pulse propagation in temporally dispersive media - exact solutions versus numerical results*. (Technical Report LUTEDX/(TEAT-7053)/1-35/(1997); Vol. TEAT-7053). [Publisher information missing].

Total number of authors:
1

General rights
Unless other specific re-use rights are stated the following general rights apply:
Copyright and moral rights for the publications made accessible in the public portal are retained by the authors and/or other copyright owners and it is a condition of accessing publications that users recognise and abide by the legal requirements associated with these rights.
• Users may download and print one copy of any publication from the public portal for the purpose of private study or research.
• You may not further distribute the material or use it for any profit-making activity or commercial gain
• You may freely distribute the URL identifying the publication in the public portal

Read more about Creative commons licenses: https://creativecommons.org/licenses/

Take down policy
If you believe that this document breaches copyright please contact us providing details, and we will remove access to the work immediately and investigate your claim.

LUND UNIVERSITY

PO Box 117
221 00 Lund
+46 46-222 00 00

CODEN:LUTEDX/(TEAT-7053)/1-35/(1997)

One-dimensional pulse propagation in temporally dispersive media — exact solutions versus numerical results

Sten Rikte

Department of Electroscience
Electromagnetic Theory
Lund Institute of Technology
Sweden

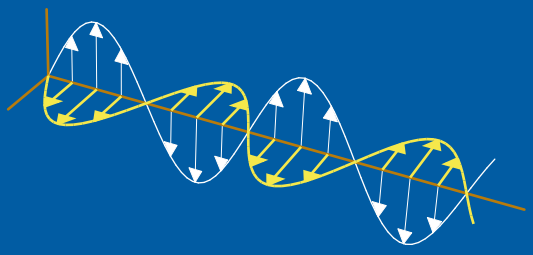

Sten Rikte

Department of Electromagnetic Theory
Lund Institute of Technology
P.O. Box 118
SE-221 00 Lund
Sweden

Editor: Gerhard Kristensson
© Sten Rikte, Lund, January 10, 1997

Abstract

One-dimensional pulse propagation in temporally dispersive dielectrics is analyzed using a scalar, causal fundamental solution of the dispersive wave operator (a single, retarded Green's function). A number of exact solutions for normal incidence on dispersive half-spaces are given, and these solutions are compared to time-domain numerical results and to forerunners (precursors).

1 Introduction

One-dimensional propagation of pulses in homogeneous, temporally dispersive, isotropic dielectrics has been analyzed in a great number of publications using both traditional methods and time-domain techniques, see Refs 2, 12, 13, 17 for some of the most significant results. The traditional methods are based on temporal Fourier transformation and advanced saddle-point analysis [17]. Usually, the frequency analysis is restricted to some special medium, e.g., the single-resonance Lorentz medium. The time-domain methods often stress the general aspects of material dispersion 2, 12, 13. There are, at least, three different, but intimately related, time-domain methods that rely on so called optical wave splitting: the imbedding method [2], the Green functions method [13], and the propagator method [10]. These methods are applicable to stratified media as well. For homogeneous media, there is also a time-domain method based on dispersive wave splitting [12]. This method is no doubt the most attractive of the time-domain methods both in the theoretical and the numerical sense.

In the present paper, the interest is focused on exact solutions at plane-wave pulse propagation in homogeneous, temporally dispersive media. Relevant time-domain properties are the refractive kernel, $N(t)$, the impedance kernel, $Z(t)$, and the propagator kernel, $P(|z|;t)$. At normal incidence on a dispersive half-space, the reflection kernel, $R(t)$, is of interest as well. For slab problems, the reflection and transmission kernels can be expressed in terms of the kernels $P(|z|;t)$ and $R(t)$, see Ref. 12. Exact solutions of these pulse propagation problems are useful for several reasons:

- An heuristic understanding of pulse propagation in dispersive, absorbing media may be gained. This is important since most media of interest are dispersive.
- The potential of traditional and novel numerical algorithms for solving pulse propagation problems in dispersive media may be investigated.
- Traditional and novel techniques to obtain forerunners (precursors) may be checked. This is an important point since numerical methods very well may fail or may be found to be very time- and/or memory-consuming for propagation distances as short as one micrometer.

The Lorentz model and the Debye model seem to be the most frequently used models for material, temporal dispersion, see, e.g., Chelkowski [5, pp. 83-110] and Kristensson [13]. The Lorentz model or the resonance model is appropriate for

many solids and both single-resonance and multiple-resonance cases are discussed in the literature. The Debye model or the relaxation model is employed to describe dispersion in polar liquids such as water and alcohols for applications in the microwave regime. Both single-relaxation models and double-relaxation models have been employed, see, e.g., Liebe *et al.* [15]. A third group of dispersive materials is Debye-Lorentz media, which, to some accuracy, describe the dynamic of the charges in the cold plasma, see, e.g., Dvorak and Dudley [6]. The Debye-Lorentz model can be considered in the perspective of making the Debye model compatible with microscopic arguments. A fourth group of media is described by the Drude dispersion model, which takes conductivity into consideration. It should be noted that results for the Debye-Lorentz model and for the Drude model can be obtained as limit cases of the results for the Lorentz model, see Section 2.

It seems hard to obtain exact solutions to pulse propagation problems in materials defined by the common dispersion models. In this paper, two novel groups of absorbing, temporally dispersive media are introduced. The first group resembles to Debye media and is referred to as modified Debye media. The second group resembles to Lorentz media and is called modified Lorentz media. For these groups of materials, one-dimensional pulse propagation problems are exactly solvable. Some results for Debye media, double-Debye media, Lorentz media, double-Lorentz media, Debye-Lorentz media, and conducting media are given as well. Several of these results can be found in the literature, see, e.g., Refs 2, 7, 21. In this article, they are collected in a general context.

In Section 2, the basic theory of material, temporal dispersion is recapitulated and the most commonly used models for such dispersion are presented. In Section 3, the time-domain index of refraction and intrinsic impedance are introduced and the results for the common models presented. Scalar, causal fundamental solutions of one-dimensional first-order and second-order dispersive wave operators are introduced in section 4. In Section 5, normal incidence at a plane nondispersive-dispersive interface is discussed. Reflection kernels are introduced and the results for the common models presented. Sommerfeld's and Brillouin's forerunners are reviewed in Section 6. In Section 7, exact expressions for the refractive kernels, the impedance kernels, and the reflection kernels are compared to numerical results in several different cases. The propagator kernels are compared to the forerunners. The two novel dispersion models are presented in Section 8. Exact expressions for the characteristic kernels of these media are presented and compared to numerical results and to precursors.

2 Common models for dispersive dielectrics

Throughout this article, Cartesian coordinates $O(x, y, z)$ are used. The radius vector is written $\boldsymbol{r} = \boldsymbol{u}_x x + \boldsymbol{u}_y y + \boldsymbol{u}_z z$, where $\boldsymbol{u}_x$, $\boldsymbol{u}_y$, and $\boldsymbol{u}_z$ are the basis vectors in the $x-$direction, $y-$direction, and $z-$direction, respectively. Time is denoted by t.

The electric and magnetic field intensities at $(\boldsymbol{r}, t)$ are denoted by $\boldsymbol{E}(\boldsymbol{r}, t)$ and $\boldsymbol{H}(\boldsymbol{r}, t)$, respectively, and the corresponding flux densities are $\boldsymbol{D}(\boldsymbol{r}, t)$ and $\boldsymbol{B}(\boldsymbol{r}, t)$.

Each field vector is written in the form

$$\boldsymbol{E} = \boldsymbol{u}_x E_x(\boldsymbol{r}, t) + \boldsymbol{u}_y E_y(\boldsymbol{r}, t) + \boldsymbol{u}_z E_z(\boldsymbol{r}, t).$$

The speed of light in vacuum is c and the intrinsic impedance of vacuum η. The Dirac delta function is denoted by $\delta(t)$ and $\delta(z)$ and the Heaviside step function by $H(t)$ and $H(z)$.

The Maxwell equations govern the dynamics of the fields in macroscopic media. The source-free Maxwell equations are

$$\nabla \times \boldsymbol{E}(\boldsymbol{r}, t) = -\partial_t \boldsymbol{B}(\boldsymbol{r}, t), \qquad \nabla \times \boldsymbol{H}(\boldsymbol{r}, t) = \partial_t \boldsymbol{D}(\boldsymbol{r}, t),$$

where the current density, $\boldsymbol{J}(\boldsymbol{r}, t)$, due to a finite conductivity has been included in the displacement current density $\partial_t \boldsymbol{D}(\boldsymbol{r}, t)$. The constitutive relations of a homogeneous, temporally dispersive, nonmagnetic, isotropic medium are

$$c\eta \boldsymbol{D}(\boldsymbol{r}, t) = [\mathcal{E}_r]\boldsymbol{E}(\boldsymbol{r}, t), \qquad c\boldsymbol{B}(\boldsymbol{r}, t) = \eta \boldsymbol{H}(\boldsymbol{r}, t), \tag{2.1}$$

where

$$\mathcal{E}_r = (\delta + \chi)* = 1 + \chi* \tag{2.2}$$

is the relative permittivity operator and the star $(*)$ denotes convolution in time:

$$(\chi * \boldsymbol{E})(\boldsymbol{r}, t) = \int_{-\infty}^{t} \chi(t - t')\boldsymbol{E}(\boldsymbol{r}, t')\, dt'.$$

The susceptibility kernel $\chi(t)$ vanishes for $t < 0$ and is assumed to be bounded and smooth for $t > 0$. This implies causality: the wave-front of any non-pathological electromagnetic field propagates through the dispersive material with the speed of light in vacuum, see Roberts [19]. No other restrictions are imposed on the medium. Recall that the susceptibility functions for dielectrics are often sensitive to temperature variations, see, e.g., Ref. 15.

In the literature, the susceptibility kernel is often required to be absolutely integrable. This property applies to absorbing, non-conducting media and admits Fourier transformation. According to the Riemann-Lesbesgue lemma, such a medium vanishes in electromagnetical sense in the high-frequency limit. Moreover, the Kramer-Kronig relations are satisfied by definition [9, p. 310]. In some references, the susceptibility kernel is required to be continuous as well [9, p. 310]; however, such a restriction excludes important media such as Debye media (and conducting media). Notice also that a discontinuous susceptibility kernel is not in conflict with causality, see Ref. 19. Finally, it is reasonable to require the medium to be dissipative, see Karlsson and Kristensson [11] for a precise definition of this concept. For dissipative dielectrics, the following result has been obtained [11]:

$$\chi(+0) = 0 \Rightarrow \chi'(+0) \geq 0 \text{ and } |\chi'(t)| \leq \chi'(+0) \text{ for } 0 \leq t < \infty. \tag{2.3}$$

It is not unusual to encounter more general constitutive relations for dispersive dielectrics than (2.1). Specifically, the relative permittivity operator (2.2) may include a so called optical response, $\mathcal{E}_r = \epsilon_r(\delta + \chi)*$, where the number $\epsilon_r \geq 1$ is

the relative permeability in the short-wave limit. The presence of an optical response does not contradict the causality concept, see Ref. 19. However, an optical response makes some important pulse propagation problems hard or impossible to solve. Two problems of this category are total reflection at oblique incidence from an electromagnetically "thicker" to an electromagnetically "thinner" medium and pulse propagation in optical fibres. Finally, it should be noted that inhomogeneities, spatial dispersion [18, p. 123], and nonlinearities [5] should be taken into consideration as well in order to obtain the proper conduct of a real dielectric.

The Debye dispersion model reads

$$\chi(t) = \alpha \exp(-\beta t) H(t),$$

where $\tau = \beta^{-1} > 0$ is the relaxation time. The susceptibility kernel is discontinuous and absolutely integrable.

The Lorentz model is specified by

$$\chi(t) = \frac{\omega_p^2}{\nu_0} \sin(\nu_0 t) \exp\Big(-\frac{\nu}{2} t\Big) H(t), \quad \nu_0 = \sqrt{\omega_0^2 - \frac{\nu^2}{4}}, \quad 0 < \frac{\nu}{2} < \omega_0,$$

where ω_0 is the natural or harmonic frequency, ω_p the plasma frequency, and ν the collision frequency. The susceptibility kernel is continuous and absolutely integrable.

The Debye-Lorentz medium

$$\chi(t) = \omega_p^2 t \exp(-\omega_0 t) H(t)$$

corresponds to the limit case $\nu/2 \nearrow \omega_0$ or $\nu_0 \searrow 0$ in the Lorentz model. The susceptibility kernel is continuous and absolutely integrable.

The Drude model for dispersive, conducting media is

$$\chi(t) = \frac{\omega_p^2}{\nu}\big(1 - \exp(-\nu t)\big) H(t).$$

This model is obtained by letting the harmonic frequency ω_0 in the Lorentz model tend to zero. The susceptibility kernel is continuous and non-integrable.

The susceptibility kernel of the simple, conducting medium is

$$\chi(t) = \sigma c \eta H(t),$$

where σ denotes conductivity. This model is a limit case of the Drude model (put $\omega_p^2 = \sigma c \eta \nu$ and let ν tend to infinity) and of the Debye model (let β tend to zero). The susceptibility kernel is discontinuous and non-integrable.

The susceptibility kernel of the plasma in the absence of an external static magnetic field is

$$\chi(t) = \omega_p^2 t H(t),$$

where ω_p is the plasma frequency. This model is a limit case of the Debye-Lorentz medium (let ω_0 tend to zero). This model also describes (non-material) modal dispersion in the closed empty wave guide (set $\omega_p = c\lambda_n$ for the mode characterized by the eigenvalue λ_n) [14]. The susceptibility kernel is continuous and non-integrable.

3 Refractive index and intrinsic impedance

In Section 2, the relative permittivity operator $\mathcal{E}_r$ was introduced, see equation (2.2). Integral operators belonging to the class (2.2) are useful since they can be multiplied without leaving the class. Obviously, the commutative and associative laws hold under such multiplication (recall the properties of the susceptibility kernel). The inverse of $\mathcal{E}_r$ can be defined uniquely within the class (2.2) as well, see Appendix A. This operator is referred to as the resolvent operator of $\mathcal{E}_r$ and is denoted by $\mathcal{E}_r^{-1}$. In the analysis of the propagation of pulses in temporally dispersive media, the integral operators $\mathcal{E}_r^{1/2}$ and $\mathcal{E}_r^{-1/2}$, which are uniquely defined within the class (2.2), arise naturally.

3.1 The refractive index of a dispersive medium

The index of refraction of a temporally dispersive, nonmagnetic dielectric is a temporal integral operator on the form

$$\mathcal{N} \equiv 1 + N*, \quad \text{where} \quad \mathcal{N}^2 = \mathcal{E}_r. \tag{3.1}$$

The refractive index corresponds to the complex index of refraction as a function of angular frequency, see Brillouin [4, p. 43], Jackson [9, p. 328], and Oughstun and Sherman [17, p. 23], and determines the propagation operators of the medium, see Section 4.

The kernel of the index of refraction, $N(t)$, satisfies the non-linear Volterra integral equation of the second kind

$$2N(t) + (N * N)(t) = \chi(t). \tag{3.2}$$

This equation has a unique solution in the space of bounded and smooth functions in each bounded time interval $0 < t < T$. Explicitly, the refractive kernel can be written in the form

$$N(t) = \sum_{k=1}^{\infty} \binom{\frac{1}{2}}{k} \left((\chi*)^{k-1}\chi\right)(t).$$

The refractive kernel vanishes for $t < 0$ and has a finite jump-discontinuity at $t = 0$ if and only if the susceptibility kernel has such a discontinuity: $N(+0) = \chi(+0)/2$. In the numerical examples in Section 7 and Section 8, equation (3.2) is used to compute the refractive kernel.

For the Debye medium, the refractive kernel is

$$N(t) = \frac{\alpha}{2}\left(I_0\left(\frac{\alpha}{2}t\right) + I_1\left(\frac{\alpha}{2}t\right)\right)\exp\left(-\gamma t\right)H(t), \tag{3.3}$$

where $I_n(x)$ are modified Bessel functions and

$$\gamma = \beta + \frac{\alpha}{2}. \tag{3.4}$$

For the Lorentz medium, the corresponding result is

$$N(t) = \left(a_{\nu_0} H(t) + \left(A_{\nu_0} H * C_\omega H\right)(t)\right) \exp\left(-\frac{\nu}{2} t\right), \tag{3.5}$$

where

$$\omega = \sqrt{\nu_0^2 + \omega_p^2} \tag{3.6}$$

and the functions $A_f(t)$, $a_f(t)$, and $C_f(t)$ for arbitrary frequency f are defined in Appendix B. For the Debye-Lorentz medium, the refractive kernel is

$$N(t) = \left(\int_0^t \frac{\omega_p^2}{2} \left(J_0(\omega_p t) + J_2(\omega_p t) \right) dt \right) \exp(-\omega_0 t) H(t),$$

where $J_n(x)$ are Bessel functions of the first kind. All these results are easy to obtain by Laplace transform technique.

Another example is given by a medium characterized by two Debye models with different relaxation times $\beta_1^{-1} \geq 0$ and $\beta_2^{-1} \geq 0$:

$$\chi(t) = \alpha_1 \exp(-\beta_1 t) H(t) + \alpha_2 \exp(-\beta_2 t) H(t), \qquad \beta_1 > \beta_2. \tag{3.7}$$

The strengths $\alpha_1 \geq 0$ and $\alpha_2 \geq 0$ are arbitrary. This model is appropriate for (liquid) water in the frequency range 0–1 THz [15]. The refractive kernel for the double-Debye medium can be written in the form

$$N(t) = N^+(t) + N^-(t) + \left(N^+ * N^-\right)(t),$$

where

$$N^+(t) = a^+ \left(I_0\left(a^+ t\right) + I_1\left(a^+ t\right)\right) \exp\left(-a^+ t\right) \exp(-\beta_1 t) H(t),$$
$$N^-(t) = a^- \left(I_0\left(a^- t\right) + I_1\left(a^- t\right)\right) \exp\left(-a^- t\right) \exp(-\beta_2 t) H(t),$$

and

$$0 \leq 4a^+ = \alpha_1 - \beta_1 + \alpha_2 + \beta_2 + \sqrt{(\alpha_1 - \beta_1 + \alpha_2 + \beta_2)^2 + 4\alpha_1(\beta_1 - \beta_2)},$$
$$0 \leq 4a^- = \alpha_1 + \beta_1 + \alpha_2 - \beta_2 - \sqrt{(\alpha_1 + \beta_1 + \alpha_2 - \beta_2)^2 - 4\alpha_2(\beta_1 - \beta_2)}.$$

This result can be obtained by Laplace transform technique. Observe that the arguments of the square roots are equal and non-negative. Notice also that a^- tends to zero and a^+ to $(\alpha_1 + \alpha_2)/2$ when $\beta_1 - \beta_2$ approaches zero in concordance with equation (3.3).

Finally, the refractive kernel for the double-resonance Lorentz medium is investigated. This medium exhibits two Lorentz processes:

$$\chi(t) = \frac{\omega_{p1}^2}{\nu_{01}} \sin(\nu_{01} t) \exp\left(-\frac{\nu_1}{2} t\right) H(t) + \frac{\omega_{p2}^2}{\nu_{02}} \sin(\nu_{02} t) \exp\left(-\frac{\nu_2}{2} t\right) H(t). \tag{3.8}$$

For simplicity, the collision frequencies are assumed to be equal ($\nu_1 = \nu_2 = \nu$). The refractive index can be expressed in terms of convolutions of the functions introduced in Appendix B:

$$\begin{aligned} N(t)\exp(\nu t/2) = a_{\nu_{01}}(t)H(t) + a_{\nu_{02}}(t)H(t) + (a_{\nu_{01}}H * a_{\nu_{02}}H)(t) + \\ + (A_{\nu_{01}}H * A_{\nu_{02}}H * C_{a^+}H * C_{a^-}H)(t) + \\ + \frac{d}{dt}(A_{\nu_{01}}H * A_{\nu_{02}}H * (C_{a^+}H + C_{a^-}H))(t), \end{aligned}$$

where the frequencies $a^{\pm} \geq 0$ are

$$a^{\pm} = \sqrt{\frac{\nu_{01}^2 + \nu_{02}^2 + \omega_{p1}^2 + \omega_{p2}^2 \pm \sqrt{\left(\nu_{01}^2 - \nu_{02}^2 + \omega_{p1}^2 - \omega_{p2}^2\right)^2 + 4\omega_{p1}^2\omega_{p2}^2}}{2}}.$$

Notice that a^- tends to zero and a^+ to $\sqrt{\nu_{01}^2 + \omega_{p1}^2}$ when ν_{02} and ω_{p2} approach zero in concordance with equation (3.5). The result in the general case is lengthy and hardly useful.

3.2 The intrinsic impedance of a dispersive medium

The intrinsic impedance of a temporally dispersive, nonmagnetic dielectric is a temporal integral operator on the form

$$\mathcal{Z} \equiv \eta(1 + Z*), \quad \text{where} \quad \mathcal{Z}^2/\eta^2 = \mathcal{E}_r^{-1}. \tag{3.9}$$

The intrinsic impedance affects the source-term in the dispersive wave equation, see Section 4. It corresponds to the complex intrinsic impedance of the medium as a function of angular frequency [17, p. 38]. The kernel of the intrinsic impedance, $Z(t)$, satisfies the non-linear Volterra integral equations of the second kind

$$\chi + 2\chi * Z + \chi * Z * Z + 2Z + Z * Z = 0, \qquad 2Z + Z * Z = \chi_{\text{res}},$$

where the resolvent kernel, $\chi_{\text{res}}(t)$ is defined in Appendix A. These equations have unique solutions in the space of bounded and smooth functions in each bounded time interval $0 < t < T$. The impedance kernel vanishes for $t < 0$ and has a finite jump-discontinuity at $t = 0$ if and only if the susceptibility kernel has such a discontinuity: $Z(+0) = -\chi(+0)/2$.

Observe that the fact that the medium is nonmagnetic can be used to obtain the intrinsic impedance kernel (combine definitions (3.1) and (3.9)):

$$N(t) + Z(t) + (Z * N)(t) = 0. \tag{3.10}$$

In other words, $Z(t)$ is the resolvent kernel of $N(t)$. In the numerical examples in Section 7 and Section 8, equation (3.10) is used to compute the impedance kernel.

For the Debye medium, the intrinsic impedance kernel is

$$Z(t) = -\frac{\alpha}{2}\left(I_0\left(\frac{\alpha}{2}t\right) - I_1\left(\frac{\alpha}{2}t\right)\right)\exp(-\gamma t)H(t),$$

where the frequency γ is given by equation (3.4). For the single-resonance Lorentz medium, the corresponding result is

$$Z(t) = \left(a_\omega(t)H(t) + \left(A_\omega H * C_{\nu_0} H\right)(t)\right) \exp\left(-\frac{\nu}{2}t\right),$$

where the functions $A_f(t)$, $a_f(t)$, and $C_f(t)$ are given by equations (B.1)–(B.3) and the frequency ω by equation (3.6). For the Debye-Lorentz medium, the intrinsic impedance kernel is

$$Z(t) = -\omega_p J_1(\omega_p t) \exp(-\omega_0 t) H(t).$$

These results are easily obtained using the resolvent kernels in Appendix A. Similarly, the impedance kernel corresponding to the double-Debye medium (3.7) and the double-Lorentz medium (3.8) can be calculated using the resolvent kernels (A.1) and (A.2), respectively.

4 Scalar, causal fundamental solutions for dispersive wave operators in one dimension

The simplest radiation problem for an unbounded, dispersive dielectric with the constitutive relations (2.1) is to calculate the electromagnetic response to a transverse current source distribution:

$$\boldsymbol{J}(\boldsymbol{r}, t) = \boldsymbol{J}(z, t) = \boldsymbol{u}_x J_x(z, t) + \boldsymbol{u}_y J_y(z, t).$$

This distribution, which is assumed to be an initially quiescent, bounded, and smooth function of time and an integrable function of the longitudinal spatial variable, supports transverse electric and magnetic (TEM) waves:

$$\begin{aligned} \boldsymbol{E}(\boldsymbol{r}, t) &= \boldsymbol{E}(z, t) = \boldsymbol{u}_x E_x(z, t) + \boldsymbol{u}_y E_y(z, t), \\ \boldsymbol{H}(\boldsymbol{r}, t) &= \boldsymbol{H}(z, t) = \boldsymbol{u}_x H_x(z, t) + \boldsymbol{u}_y H_y(z, t). \end{aligned} \tag{4.1}$$

The Maxwell equations are

$$\nabla \times \boldsymbol{E} = -c^{-1}\partial_t(\eta \boldsymbol{H}), \qquad \nabla \times (\eta \boldsymbol{H}) = c^{-1}\partial_t(1 + N*)^2 \boldsymbol{E} + \eta \boldsymbol{J}$$

or

$$\partial_z \boldsymbol{E} = c^{-1}\partial_t\left(\boldsymbol{u}_z \times \eta \boldsymbol{H}\right), \qquad \partial_z\left(\boldsymbol{u}_z \times \eta \boldsymbol{H}\right) = \eta \boldsymbol{J} + c^{-1}\partial_t \mathcal{E}_r \boldsymbol{E}. \tag{4.2}$$

The task is to obtain scalar, causal fundamental solutions of first-order and second-order dispersive wave operators.

4.1 The second-order wave operator

The combination of the Maxwell equations gives the dispersive wave equation for the electric field:

$$\frac{1}{2}c\partial_t^{-1}(1+N*)^{-1}\left(-\partial_z^2+c^{-2}\partial_t^2(1+N*)^2\right)\boldsymbol{E}=-\frac{1}{2}\eta(1+Z*)\boldsymbol{J}. \tag{4.3}$$

The solution of this propagation problem can be given in terms of the retarded fundamental solution of the dispersive wave operator

$$\frac{1}{2}c\partial_t^{-1}(1+N*)^{-1}\left(-\partial_z^2+c^{-2}\partial_t^2(1+N*)^2\right). \tag{4.4}$$

This solution is denoted by $\mathcal{E}(|z|,t)$ and satisfies the wave equation

$$\left(-\partial_z^2+c^{-2}\partial_t^2(1+N*)^2\right)\mathcal{E}(|z|,t)=\delta(z)2c^{-1}\partial_t(1+N*)\,\delta(t). \tag{4.5}$$

The dispersive fundamental solutions play the same role for the dispersive wave operators as the fundamental solutions do for the differential operators with constant coefficients; thus, the solution of the dispersive wave equation (4.3) is

$$\boldsymbol{E}(z,t)=-\frac{1}{2}\int\Big(\int\mathcal{E}(|z-z'|;t-t')(\mathcal{Z}\boldsymbol{J})(z',t')\;dt'\Big)\;dz'. \tag{4.6}$$

Formally, this fact is easily proven by letting the dispersive wave operator (4.4) operate under the integral signs. Under suitable assumptions, the integral representation (4.6) is a consequence of Schwartz' kernel theorem [8, pp. 128-129]. Having obtained the electric field, Faraday's law yields the corresponding magnetic field:

$$\boldsymbol{H}(z,t)=-\frac{1}{2}\int\Big(\int\operatorname{sgn}(z-z')\mathcal{E}(|z-z'|;t-t')\boldsymbol{u}_z\times\boldsymbol{J}(z',t')\;dt'\Big)\;dz',$$

where $\operatorname{sgn}(z)$ is the sign function: $\operatorname{sgn}(z)=-1$ for $z<0$ and $\operatorname{sgn}(z)=+1$ for $z>0$.

The retarded fundamental solution of the dispersive wave operator is defined in the following theorem.

Theorem 4.1. *The distribution*

$$\mathcal{E}(|z|;t)=Q(|z|)\Big(\delta\left(t-|z|/c\right)+P\left(|z|;t-|z|/c\right)\Big), \tag{4.7}$$

where the wave-front propagator, $Q(|z|)$, satisfies the ordinary differential equation

$$c\partial_{|z|}Q(|z|)=-N(+0)Q(|z|),\qquad Q(0)=1, \tag{4.8}$$

and the propagator kernel, $P(|z|;t)$, satisfies the integro-differential equation

$$c\partial_{|z|}P(|z|;t)=-N'(t)-\big(N'(\cdot)*P(|z|;\cdot)\big)(t),\qquad P(0;t)=0, \tag{4.9}$$

is a causal or retarded fundamental solution of the dispersive wave operator (4.4).

Observe that $P(|z|;t) = P(0;t) = 0$ for $t < 0$; consequently $\mathcal{E}(|z|;t) = 0$ for $t < |z|/c$, that is, the fundamental solution $\mathcal{E}(|z|;t)$ is causal. Notice also that the well known result for out-going waves in vacuum is obtained from equation (4.7) by setting $N = 0$: $\mathcal{E}(|z|;t) = \delta\,(t - |z|/c)$.

Two brief proofs of Theorem 4.1 are given:

Proof. Differentiating equation (4.7) and using equation (4.8), equation (4.9) and the identity

$$\partial_{|z|}\delta\,(t - |z|/c) = -c^{-1}\partial_t\delta\,(t - |z|/c)\,,$$

give an integro-differential equation for $\mathcal{E}\,(z;t)$:

$$\partial_{|z|}\mathcal{E} = -c^{-1}\partial_t(1 + N*)\mathcal{E}, \qquad \mathcal{E}(0;t) = \delta(t). \tag{4.10}$$

Differentiating this result with respect to z and using the identity

$$\partial_z^2\delta\,(t - |z|/c) = c^{-2}\partial_t^2\delta\,(t - |z|/c) - \delta(z)2c^{-1}\partial_t\delta(t)$$

yield the desired result.

Alternative proof. In this proof, it is assumed that the fundamental solution is a temperated distribution with respect to time. Temporal Fourier transform of equation (4.10) gives $\mathcal{E}(|z|;\omega) = \exp\left(-ik(\omega)\,|z|\right)$, where $k(\omega) = \omega n(\omega)/c$ is the complex wave number and $n(\omega) = 1 + N(\omega)$ the complex refractive index. In the Fourier space, the dispersive fundamental equation (4.5) reduces to the ordinary differential equation $-\left(\partial_z^2 + k^2(\omega)\right)\mathcal{E}(|z|;\omega) = 2ik(\omega)\delta(z)$. It is straightforward to see that $\mathcal{E}(|z|;\omega) = \exp\left(-ik(\omega)\,|z|\right)$ satisfies this equation. This finishes the proof.

Equation (4.10) shows that the wave number

$$\mathcal{K} = c^{-1}\partial_t\mathcal{N} = c^{-1}\partial_t(1 + N*) = (c^{-1}\partial_t\delta + c^{-1}N(+0)H + K)*, \quad K(t) = c^{-1}N'(t)$$

is a relevant integro-differential operator for pulse propagation in dispersive media. In terms of the wave number, equation (4.10) reads $\partial_{|z|}\mathcal{E} = -\mathcal{K}\mathcal{E}$. In the time-harmonic analysis, the wave number $\mathcal{K}$ corresponds to the complex wave number [17, p. 38].

4.2 Properties of the fundamental solution

The wave-front propagator, $Q(|z|)$, can be calculated explicitly:

$$Q(|z|) = \exp\left(-\frac{|z|}{c}N(+0)\right). \tag{4.11}$$

A closed-form expression for the propagator kernel, $P(|z|;t)$, cannot be obtained in general. However, the propagator kernel can be represented by the infinite series

$$P(|z|;t) = \sum_{k=1}^{\infty}\frac{(-|z|)^k}{k!}\left((K*)^{k-1}K\right)(t), \tag{4.12}$$

which converges uniformly in each bounded time-interval. Since the wave-number kernel, $K(t)$, is bounded and smooth in each bounded time-interval, $P(|z|;t)$ inherits

these properties. Numerically, a temporal integral equation of the second kind can be solved for the propagator kernel:

$$tP = -|z|tK - |z|(tK) * P, \quad P(|z|;+0) = -|z|K(+0). \tag{4.13}$$

This equation is of second order Volterra type and therefore stable. The integral equation (4.13), can be derived using the general identity for causal convolutions

$$t\frac{\overbrace{(f*\ldots*f)}^{k \text{ functions}}}{k!} = (tf) * \frac{\overbrace{(f*\ldots*f)}^{k-1 \text{ functions}}}{(k-1)!}, \qquad k>1,$$

which, in turn, is proved by mathematical induction. In the numerical examples in Section 7 and Section 8, either the series expansion (4.12) or the integral equation (4.13) is employed.

Transient phenomena at one-dimensional wave-propagation in temporally dispersive media are completely determined by the fundamental solution $\mathcal{E}(|z|;t)$. Unfortunately, fundamental solutions of the wave operators for Debye, Lorentz, and Debye-Lorentz media are hard to obtain analytically. However, the non-absorbing Debye medium $\chi(t) = \alpha H(t)$ is an exception:

$$\mathcal{E}(|z|;t) = \frac{|z|}{ct}\left(\frac{d}{dt}+\frac{\alpha}{2}\right)\left(I_0\left(\frac{\alpha}{2}\sqrt{t^2-\frac{z^2}{c^2}}\right)\exp\left(-\frac{\alpha}{2}t\right)H\left(t-\frac{|z|}{c}\right)\right)$$

or

$$\begin{aligned}\mathcal{E}(|z|;t) = {} & \exp\left(-\frac{\alpha|z|}{2c}\right)\delta\left(t-\frac{|z|}{c}\right) + \\ & + \frac{\alpha^2|z|}{8c}\left(I_0\left(\frac{\alpha}{2}\sqrt{t^2-\frac{z^2}{c^2}}\right) - I_2\left(\frac{\alpha}{2}\sqrt{t^2-\frac{z^2}{c^2}}\right)\right)\exp\left(-\frac{\alpha}{2}t\right)H\left(t-\frac{|z|}{c}\right).\end{aligned}$$

This result follows easily by differentiating the Laplace transform

$$\mathcal{E}(|z|;t) \longleftrightarrow \exp\left(-\frac{|z|}{c}\sqrt{s(s+\alpha)}\right)$$

with respect to the Laplace parameter s, see Abramowitz and Stegun [1]. This is the response from a simple, conducting medium with conductivity $\sigma = \alpha/(c\eta)$, see, e.g., Stratton [21, p. 320].

Similarly, by differentiating the Laplace transform

$$\mathcal{E}(|z|;t) \longleftrightarrow \exp\left(-\frac{|z|}{c}\sqrt{s^2+\omega_p^2)}\right)$$

with respect to the Laplace parameter s, the fundamental solution of the non-absorbing modified Debye-Lorentz medium $\chi(t) = \omega_p^2 tH(t)$ can be obtained exactly:

$$\begin{aligned}\mathcal{E}(|z|;t) = {} & \frac{|z|}{ct}\frac{d}{dt}\left(J_0\left(\omega_p\sqrt{t^2-\frac{z^2}{c^2}}\right)H\left(t-\frac{|z|}{c}\right)\right) = \\ & = \delta\left(t-\frac{|z|}{c}\right) - \frac{\omega_p^2|z|}{2c}\left(J_0\left(\omega_p\sqrt{t^2-\frac{z^2}{c^2}}\right) + J_2\left(\omega_p\sqrt{t^2-\frac{z^2}{c^2}}\right)\right)H\left(t-\frac{|z|}{c}\right).\end{aligned}$$

This fundamental solution is relevant for propagation of radio waves in the ionized layers of the atmosphere, where the mean free path of the electrons is exceedingly long, see, e.g., Felsen and Marcuvitz [7, p. 163] or Dvorak and Dudley [6]. Furthermore, it appears at mode propagation in the empty waveguide, see Kristensson [14].

4.3 First-order wave operators

Wave operators for the up-going and the down-going fields can be derived directly from the first-order system (4.2) using a dispersive wave-splitting. The split vector fields, $\boldsymbol{E}^{\pm}(z,t)$, are defined by

$$\boldsymbol{E}^{\pm} = \frac{1}{2}\left(\boldsymbol{E} \mp \mathcal{Z}\boldsymbol{u}_z \times \boldsymbol{H}\right). \tag{4.14}$$

In terms of these fields, the electric and magnetic field strengths are

$$\boldsymbol{E} = \boldsymbol{E}^{+} + \boldsymbol{E}^{-}, \qquad \boldsymbol{u}_z \times \eta\boldsymbol{H} = -\mathcal{N}\boldsymbol{E}^{+} + \mathcal{N}\boldsymbol{E}^{-}.$$

Subject to the transformation (4.14), the Maxwell equations (4.2) reduce to the dynamical equations

$$\partial_z \boldsymbol{E}^{\pm} = \mp\mathcal{K}\boldsymbol{E}^{\pm} \mp \mathcal{Z}\boldsymbol{J}/2. \tag{4.15}$$

Consequently, $\boldsymbol{E}^{+}$ represents the up-going electric field and $\boldsymbol{E}^{-}$ the down-going electric field in the dispersive medium.

The fundamental solutions, $\mathcal{E}^{\pm}(z;t)$, of the dispersive wave operators, $\pm\partial_z + \mathcal{K}$, respectively, satisfy the first-order dispersive wave equations

$$\left(\pm\partial_z + \mathcal{K}\right)\mathcal{E}^{\pm} = \delta(z)\ \delta(t).$$

Under suitable assumptions, Schwartz' kernel theorem [8, pp. 128-129] is applicable, and the solutions of the propagation problems (4.15) can be written in the form

$$\boldsymbol{E}^{\pm}(z,t) = -\frac{1}{2}\int\left(\int \mathcal{E}^{\pm}(z-z';t-t')(\mathcal{Z}\boldsymbol{J})(z',t')\,dt'\right)dz'.$$

It is straightforward to show that the fundamental solutions, $\mathcal{E}^{\pm}(z;t)$, are

$$\mathcal{E}^{\pm}(z;t) = H\left(\pm z\right)\mathcal{E}(|z|;t),$$

where $\mathcal{E}(|z|;t)$ is defined in Theorem 4.1. The up-going and down-going magnetic fields are

$$\boldsymbol{H}^{\pm}(z,t) = \pm\boldsymbol{u}_z \times \mathcal{N}\boldsymbol{E}^{\pm}/\eta = \mp\frac{1}{2}\int\left(\int \mathcal{E}^{\pm}(z-z';t-t')\boldsymbol{u}_z \times \boldsymbol{J}(z',t')\ dt'\right)dz',$$

respectively.

In Section 5, the special case when the current source is distributed over the plane $z = 0$ is referred to. In this case, $\boldsymbol{J}(z,t) = \boldsymbol{j}_0(t)\delta(z)$. The electric fields then satisfy the dispersive first-order equations

$$\left(\pm\partial_z + c^{-1}\partial_t(1+N*)\right)\boldsymbol{E}^{\pm}(z,t) = \boldsymbol{E}_0(t)\delta(z), \tag{4.16}$$

where $\boldsymbol{E}_0 = -\eta(1 + Z*)\boldsymbol{j}_0/2$ is the electric field in the plane $z = 0$. Consequently, a current distributed over the plane $z = 0$ induces electric and magnetic fields given by

$$\begin{aligned} \boldsymbol{E}^{\pm}(z,t) &= \int \mathcal{E}^{\pm}(z, t-t')\boldsymbol{E}_0(t')\,dt', \\ \boldsymbol{H}^{\pm}(z,t) &= \mp \int \mathcal{E}^{\pm}(z; t-t')\boldsymbol{H}_0(t')dt', \end{aligned} \tag{4.17}$$

where $(1 + Z*)\eta\boldsymbol{H}_0 = \boldsymbol{u}_z \times \boldsymbol{E}_0$.

4.4 Propagation operators

In this subsection, the problem with a current distributed over the plane $z = 0$ is analyzed further. Due to symmetry, it is sufficient to study the solution in the upper half-space. Suppressing the general time-dependence, the solution (4.17) is

$$\boldsymbol{E}(z) = \mathcal{P}(z,0)\boldsymbol{E}(+0), \quad z > 0,$$

where the propagation operator,

$$\mathcal{P}(z,0) = \mathcal{E}(z,\cdot)*,$$

satisfies the operator equation

$$\partial_z\mathcal{P}(z,0) = -\mathcal{K}\mathcal{P}(z,0), \quad z > 0, \qquad \mathcal{P}(0,0) = 1.$$

The propagation operator can be written in the form

$$\mathcal{P}(z,0) = \exp(-z\mathcal{K}) = \delta_{z/c} * Q(z)\big(1 + P(z;\cdot) * \big), \tag{4.18}$$

where $\delta_{z/c} = \delta(t - z/c)$ the time-delayed Dirac pulse, $Q(z)$ is the wave-front propagator, and $P(z;t)$ the propagator kernel, see Theorem 4.1.

The propagation operator takes the field at $z = 0$ to the field at $z > 0$. More generally, a propagation operator $\mathcal{P}(z_2, z_1)$, which relates the field at $z_1 \geq 0$ to the field at $z_2 \geq 0$, can be defined. The characteristic of the exponential,

$$\mathcal{P}(z_3, z_1) = \mathcal{P}(z_3, z_2)\mathcal{P}(z_2, z_1), \qquad 0 \leq z_1 \leq z_2 \leq z_3, \tag{4.19}$$

holds for this operator. In other words,

$$\mathcal{E}(z_3 - z_1; t) = \left(\mathcal{E}(z_3 - z_2;\cdot) * \mathcal{E}(z_2 - z_1;\cdot)\right)(t).$$

or

$$P(z_3 - z_1; t) = P(z_3 - z_2; t) + P(z_2 - z_1; t) + \left(P(z_3 - z_2;\cdot) * P(z_2 - z_1;\cdot)\right)(t).$$

This rule is employed in the numerical examples below.

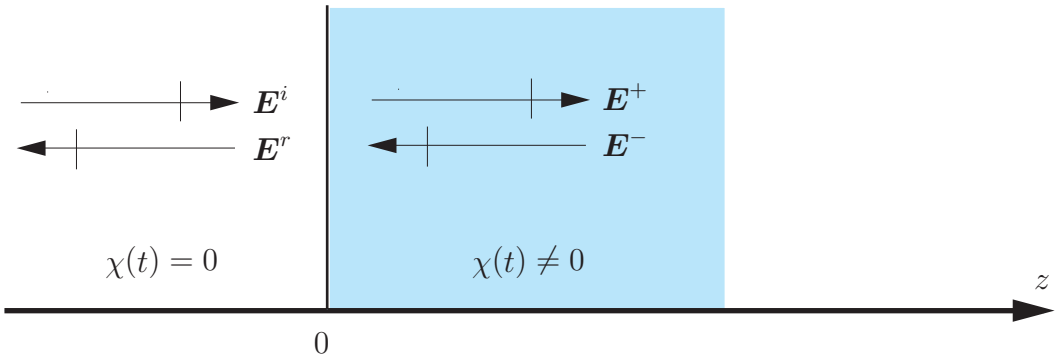

Figure 1: The scattering geometry with the incident, reflected, and split electric fields indicated. Using the dispersive wave splitting, the down-going field in the dispersive half-space is zero.

5 Normal incidence on a dispersive half-space

A linearly polarized, electromagnetic pulse is incident normally on a plane interface separating a simple, isotropic medium from a temporally dispersive, nonmagnetic dielectric. For the sake of simplicity, the non-dispersive region, $z < 0$, is assumed to be vacuum. The constitutive relations of the dispersive region, $z > 0$, are given by equation (2.1). The scattering geometry is depicted in Figure 1.

The incident electric field at the interface $z = 0$ at time t is denoted by $\boldsymbol{E}^i(t)$. This field is assumed to be initially quiescent, bounded, and smooth. By definition, the other incident field components at the interface are

$$c\eta \boldsymbol{D}^i(t) = \boldsymbol{E}^i(t), \qquad \eta \boldsymbol{H}^i(t) = c\boldsymbol{B}^i(t) = \boldsymbol{u}_z \times \boldsymbol{E}^i(t).$$

TEM wave solutions (4.1) are sought. At the boundary, $z = 0$, the fields $\boldsymbol{E}(z,t)$ and $\boldsymbol{H}(z,t)$ are continuous in z.

The reflected electric field at the interface at time t is denoted by $\boldsymbol{E}^r(t)$. Since the reflected plane wave propagates in the negative z-direction, the other reflected field components at the interface are given by

$$c\eta \boldsymbol{D}^r(t) = \boldsymbol{E}^r(t), \qquad \eta \boldsymbol{H}^r(t) = c\boldsymbol{B}^r(t) = -\boldsymbol{u}_z \times \boldsymbol{E}^r(t).$$

The dispersive wave-splitting (4.14) is now applied. Due to the absence of sources in the upper half-space, $\boldsymbol{E}^- = \boldsymbol{0}$ and $\boldsymbol{E}^+ = \boldsymbol{E}$ for $z > 0$. Evidently, the upper equation (4.16) is appropriate for this problem. The boundary condition for the electric field shows that

$$\boldsymbol{E}^+(z,t) = \int \mathcal{E}^+(z, t-t')\boldsymbol{E}^+(+0,t')\,dt', \qquad \boldsymbol{E}^+(+0,t) = \boldsymbol{E}^i(t) + \boldsymbol{E}^r(t),$$

cf equation (4.17). Suppressing the general time-dependence, the propagating electric field can be written in the form

$$\boldsymbol{E}^+(z) = \mathcal{P}(z,0)\boldsymbol{E}^+(+0), \qquad z > 0,$$

where the propagation operator, $\mathcal{P}(z,0)$, was defined in Section 4.

The Schwartz' kernel theorem [8, pp. 128-129] shows that the solution of the reflection problem can be written in the form $\boldsymbol{E}^r = \mathcal{R}\boldsymbol{E}^i = R * \boldsymbol{E}^i$, where the reflection kernel, $R(t)$, is independent of the excitation, $\boldsymbol{E}^i(t)$, and depends on the susceptibility kernel, $\chi(t)$, only. The boundary conditions show that the reflection operator is given by the operator equality

$$\mathcal{R} = \big(\mathcal{Z} + \eta\big)^{-1}\big(\mathcal{Z} - \eta\big) = \big(1 + \mathcal{N}\big)^{-1}\big(1 - \mathcal{N}\big). \tag{5.1}$$

The continuity of the electric field at the interface shows that the transmitted electric field at $z = +0$ is $\boldsymbol{E}^+(+0) = (1 + \mathcal{R})\,\boldsymbol{E}^i$. Therefore, the solution of propagation problem ($z > 0$) reads

$$\begin{aligned} &\boldsymbol{E}(z) = (1 + \mathcal{R})\mathcal{P}(z,0)\boldsymbol{E}^i, && c\eta\boldsymbol{D}(z) = (1 - \mathcal{R})\mathcal{N}\mathcal{P}(z,0)\boldsymbol{E}^i, \\ &\eta\boldsymbol{H}(z) = (1 - \mathcal{R})\mathcal{P}(z,0)\boldsymbol{u}_z \times \boldsymbol{E}^i, && c\boldsymbol{B}(z) = (1 + \mathcal{R})\mathcal{N}\mathcal{P}(z,0)\boldsymbol{u}_z \times \boldsymbol{E}^i. \end{aligned}$$

Equation (5.1) shows that $-R(t)$ is the resolvent kernel of $Z(t)/2$ and $R(t)$ is the resolvent kernel of $N(t)/2$:

$$-2R(t) + Z(t) - (Z * R)(t) = 0 = 2R(t) + N(t) + (N * R)(t). \tag{5.2}$$

Consequently, the reflection kernel vanishes for $t < 0$ and is bounded and smooth in each bounded time-interval $0 < t < T$. Substituting $\mathcal{Z}/\eta = (1 - \mathcal{R})^{-1}(1 + \mathcal{R})$ into the operator equation (3.9) yields the reflection equation

$$4R + 2\chi * R + \chi + \chi * R * R = 0, \tag{5.3}$$

which relates $R(t)$ to $\chi(t)$ directly. This equation shows that the reflection kernel has a finite jump-discontinuity at $t = 0$ if and only if $\chi(t)$ has such a discontinuity: $R(+0) = -\chi(+0)/4$. The non-linear Volterra integral equation of the second kind (5.3) is sometimes referred to as the reflection imbedding equation [2]. In the numerical examples in Section 7 and Section 8, the first equation (5.2) is employed to obtain the reflection kernel.

For the Debye medium, the reflection kernel is

$$R(t) = -\frac{1}{t} I_1\left(\frac{\alpha}{2}t\right) \exp\left(-\gamma t\right) H(t) = -\frac{\alpha}{4}\left(I_0\left(\frac{\alpha}{2}t\right) - I_2\left(\frac{\alpha}{2}t\right)\right) \exp\left(-\gamma t\right) H(t),$$

where the frequency γ is given by equation (3.4). This result has been reported by Beezley and Krueger [2]. For the Lorentz medium, the corresponding result reads

$$R(t) = \frac{2}{\omega_p^2}\big(c_\omega(t)H(t) + c_{\nu_0}(t)H(t) + \left(C_\omega H * C_{\nu_0} H\right)(t)\big) \exp\left(-\frac{\nu}{2}t\right),$$

where the functions $C_f(t)$ and $c_f(t)$ are given by equations (B.3)–(B.4) and the frequency ω by equation (3.6). Finally, for the Debye-Lorentz medium, the reflection kernel is

$$R(t) = -\frac{\omega_p}{2}\big(J_1\left(\omega_p t\right) + J_3\left(\omega_p t\right)\big) \exp\left(-\omega_0 t\right) H(t).$$

These results are easily obtained by Laplace transform technique.

6 Approximations to the propagation kernel

Sommerfeld's and Brillouin's forerunners — the first and second precursors, respectively — are the most well known transients in dispersive media [4]. Initially, these forerunners were defined for Lorentz media only [3, 20]. However, the definitions can be extended to more or less arbitrary dispersive media, see Ref. 12.

Sommerfeld's forerunner is the leading term of the wave-front behavior of the propagating field and is characterized by high oscillations in the case of a resonance medium. Brillouin's forerunner is the leading term of the slow variations of the field and arrives later than the first. The time at which this occurs is sometimes referred to as the quasilatent time.

Sommerfeld showed that the first precursor can be expressed in terms of the Bessel function J_1 with argument proportional to the square root of the propagation distance and the square root of the wave-front time. Brillouin showed that the second precursor can be expressed in terms of the Airy function Ai, with the argument depending on the propagation distance and the wave-front time in a more subtle way, see the explicit expressions below. The precursors are good approximations to the propagating field at sufficiently large propagation distances $|z|$ only. (For resonance frequencies in the optical regime, the propagation distance $z = 10^{-6}$ m is sufficiently large. For Debye media with relaxation times about $\tau = 10^{-10}$ s, the corresponding distance is approximately one meter, see Section 7 below.) In addition, Brillouin's forerunner is relevant in a neighborhood of the quasilatent time only. Corrections to the second forerunner have been obtained by Oughstun and Sherman and later by Karlsson and Rikte using different techniques, see Refs 12, 16.

Sommerfeld and Brillouin used the saddle-point method in the complex plane to obtain their results. In the present article, the time-domain approach introduced by Karlsson and Rikte is employed.

The jump in the wave-number kernel $K(t)$ at $t = 0$ generates Sommerfeld's forerunner, which is a temporal integral operator on the form (cf equation (4.18))

$$\mathcal{P}_S(z,0) = \delta_{|z|/c} * Q(|z|)\big(1 + P_S(|z|;\cdot) * \big).$$

Substituting the approximation $K(t) = K(+0)H(t)$ into the series expansion of the propagator kernel (4.12) and using the identity

$$\big((H*)^n H\big)(t) = \frac{t^n}{n!}H(t) \tag{6.1}$$

yields the forerunner kernel

$$P_S(|z|;t) = \sum_{k=1}^{\infty} \frac{(-|z|K(+0))^k}{k!}\left((H*)^{k-1}H\right)(t) = H(t)\sum_{k=1}^{\infty}\frac{(-|z|K(+0))^k}{k!}\frac{t^{k-1}}{(k-1)!}.$$

The Taylor series for Bessel functions shows that

$$\begin{aligned} P_S(|z|;t) &= -|z|K(+0)\left(I_0\left(2\sqrt{-|z|K(+0)t}\right) - I_2\left(2\sqrt{-|z|K(+0)t}\right)\right) = \\ &= -|z|K(+0)\left(J_0\left(2\sqrt{|z|K(+0)t}\right) + J_2\left(2\sqrt{|z|K(+0)t}\right)\right), \end{aligned}$$

where the first expression is appropriate for Debye media ($K(+0) < 0$) and the second for Lorentz media ($K(+0) > 0$). Thus, Sommerfeld's forerunner behaves quite differently in resonance media and in relaxation media.

Brillouin's forerunner is given by a non-causal, temporal integral operator:

$$\mathcal{P}_B(z,0) = P_B(|z|;\cdot)*,$$

where the interval of integration is $-\infty < t < +\infty$ and the kernel $P_B(|z|;t)$ is smooth in time. For relaxation media, Brillouin's forerunner kernel is given by

$$P_B(|z|;t) = \frac{1}{t_2(|z|)} B_2\left(\frac{t-|z|/c-t_1(|z|)}{t_2(|z|)}\right), \quad B_2(t) = \frac{1}{\sqrt{2\pi}}\exp\left(-\frac{t^2}{2}\right), \tag{6.2}$$

where $B_2(t)$ is the normalized Gaussian. For resonance media, the corresponding result is

$$P_B(|z|;t) = \left(\frac{1}{t_2(|z|)} B_2\left(\frac{\cdot}{t_2(|z|)}\right) * \frac{1}{t_3(|z|)} B_3\left(\frac{\cdot}{t_3(|z|)}\right)\right)(t-|z|/c-t_1(|z|)), \tag{6.3}$$

where $B_3(t) = Ai(-t)$ is the reversed Airy function. The quasilatent time is proportional to the propagation depth z and to the integral of the refractive index:

$$t_1(|z|) = |z|/c \int N(t)\, dt,$$

The scaling times, $t_2(|z|)$ and $t_3(|z|)$, are proportional the square root and the cubic root of the propagation depth, respectively, see Ref. 12 for details. Corrections to the second precursor for arbitrary resonance media can be found in Ref. 12.

7 Exact solutions versus numerical results and forerunners

In this section, exact solutions and numerical results are compared. Four examples are given: a simple conducting medium, a cold plasma, a Debye medium, and a single-resonance Lorentz medium. In the two last examples, the numerical results for the propagator kernels are compared to the forerunners.

Example 1. Normal incidence on a conducting half-space, $z > 0$.

The susceptibility kernel is $\chi(t) = \sigma c\eta H(t)$. The propagation kernel, $Q(z)P(z;t)$, at fixed propagation depth, z, for a conducting medium characterized by $\alpha = 10\times c/z$ is depicted in Figure 2. Choosing the propagation distance to be $z = 4.6\times 10^{-10}$ m, the parameter α corresponds to the conductivity of copper $\sigma = 5.81\times 10^7\,\mathrm{Ohm}^{-1}\,\mathrm{m}^{-1}$. The corresponding refractive kernel, $N(t)$, impedance kernel, $Z(t)$, and reflection kernel at normal incidence, $R(t)$, are depicted in Figure 3. Numerical results, based on the integral equation (4.13), are given for comparison.

Example 2. Normal incidence on a cold plasma half-space, $z > 0$.

The susceptibility kernel is $\chi(t) = \omega_p^2 t H(t)$. The propagation kernel, $P(z;t)$, at fixed

propagation depth, z, for a cold plasma is given in Figure 4. The Dvorak and Dudley parameters $z = 100$ m, $\omega_p = 10^7\,\mathrm{s}^{-1}$ have been used. The corresponding refractive kernel, $N(t)$, impedance kernel, $Z(t)$, and reflection kernel at normal incidence, $R(t)$, are depicted in Figure 5. Numerical results, based on the series expansion of the exponential (4.12), are given for comparison.

Example 3. Normal incidence on a Debye half-space, $z > 0$.
In this case, the susceptibility kernel is $\chi(t) = \alpha \exp(-\beta t) H(t)$. The propagation kernel, $Q(z)P(z;t)$, at fixed propagation depth, z, for a Debye half-space characterized by $\alpha = 100 \times c/z$ and $\beta = 40 \times c/z$ is depicted in Figure 6. Taking the propagation distance to be $z = 1$ m, these parameters corresponds to the relaxation time $\tau = 1/\beta = 8.33 \times 10^{-11}$ s and the strength $\alpha = 3 \times 10^{10}$ Hz. The result has been obtained numerically using series expansion of the exponential (4.12). The kernels $\chi(t)$, $N(t)$, $Z(t)$, and $R(t)$ are given in Figure 7, where exact solutions and numerical results are compared.

Figure 6 shows that the propagation kernel of the Debye medium can be approximated by the normalized Gaussian (6.2). The quasilatent time, $t_1(z)$, and the scaling time, $t_2(z)$, are given by

$$t_1(z) = \left(\sqrt{1 + \frac{\alpha}{\beta}} - 1\right) \frac{z}{c} \qquad \text{and} \qquad t_2(z) = \sqrt{\frac{1}{\sqrt{1 + \frac{\alpha}{\beta}}} \frac{\alpha}{\beta^2} \frac{z}{c}},$$

see Ref. 12.

Example 4. Normal incidence on a Lorentz half-space, $z > 0$.
The susceptibility kernel is $\chi(t) = \omega_p^2/\nu_0 \sin(\nu_0 t) \exp(-\nu/2t) H(t)$. The propagation kernel, $P(z;t)$, at fixed propagation depth, z, for a single-resonance Lorentz half-space characterized by Brillouin's parameters [4] is depicted in Figure 8 and Figure 9. The result has been obtained numerically using the integral equation (4.13). The propagator rule (4.19) was used once. Specifically, the propagation distance is $z = 10^{-6}$ m, the plasma frequency $\omega_p = \sqrt{20} \times 100/3 \times c/z$, the natural frequency $\omega_0 = 400/3 \times c/z$, and the collision frequency $\nu = 56/3 \times c/z$. Similar results have been obtained by Oughstun and Sherman in their study of forerunners [16]. Brillouin's forerunner is clearly distinguishable. The kernels $\chi(t)$, $N(t)$, $Z(t)$, and $R(t)$ are given in Figures 10–11. Exact solutions and numerical results are compared.

Figure 9 shows the wave-front behavior of the signal. Sommerfeld's forerunner is given for comparison.

Figure 8 shows that the propagation kernel of the Lorentz medium in a neighborhood of the quasilatent time can be approximated by Brillouin's forerunner (6.3). The quasilatent time, $t_1(z)$, and the scaling times, $t_2(z)$ and $t_3(z)$, are

$$t_1(z) = \left(\sqrt{1 + \frac{\omega_p^2}{\omega_0^2}} - 1\right) \frac{z}{c}, \qquad t_2(z) = \sqrt{\frac{1}{\sqrt{1 + \frac{\omega_p^2}{\omega_0^2}}} \frac{\nu \omega_p^2}{\omega_0^4} \frac{z}{c}},$$

$$t_3(z) = \left(\frac{3}{\sqrt{1 + \frac{\omega_p^2}{\omega_0^2}}} \left(\frac{\omega_p^2(\omega_0^2 - \nu^2)}{\omega_0^6} + \frac{\nu^2 \omega_p^4}{4\omega_0^8} \frac{1}{1 + \frac{\omega_p^2}{\omega_0^2}}\right) \frac{z}{c}\right)^{\frac{1}{3}},$$

see Ref. 12. In addition, the even better approximation derived in Ref. 12 is given. In the interval $0.6 < tc/z < 2$, this latter approximation almost coincides with the numerical result.

8 Modified Debye and Lorentz media

In this section, two novel groups of absorbing materials are introduced, namely, modified Debye media, which resemble Debye media, and modified Lorentz media, which are closely related to Lorentz media. For both these materials, the normal incidence problem is exactly solvable. This motivates the introduction.

8.1 The modified Debye medium

The refraction kernel of the modified Debye medium is

$$N(t) = \alpha \exp(-\beta t) H(t).$$

The corresponding susceptibility kernel is

$$\chi(t) = \left(2\alpha + \alpha^2 t\right) \exp(-\beta t) H(t),$$

the impedance kernel

$$Z(t) = -\alpha \exp(-(\alpha + \beta) t) H(t),$$

and the reflection kernel

$$R(t) = -\frac{\alpha}{2} \exp\left(-\left(\frac{\alpha}{2} + \beta\right) t\right) H(t).$$

Clearly, the dynamics of the charges in the modified Debye medium and in the Debye medium bear a close resemblance.

Straightforward computations using series expansion and the identity (6.1) show that the propagator kernel is

$$P(z;t) = a \frac{I_1\left(2\sqrt{at}\right)}{\sqrt{at}} \exp(-\beta t) H(t) = a \left(I_0\left(2\sqrt{at}\right) - I_2\left(2\sqrt{at}\right)\right) \exp(-\beta t) H(t),$$

where the frequency $a(z) = \alpha\beta z/c$. The wave-front factor is $Q(z) = \exp(-\alpha z/c)$.

The propagation kernel, $Q(z)P(z;t)$, at fixed propagation depth, z, for a modified Debye half-space characterized by $\alpha = 11 \times c/z$ and $\beta = 13 \times c/z$ is depicted in Figure 12. The numerical result has been obtained using series expansion of the exponential. The corresponding kernels $\chi(t)$, $N(t)$, $Z(t)$, and $R(t)$ are given in Figure 13. The propagation kernel, $Q(z)P(z;t)$, at fixed propagation depth, z, for a modified Debye half-space characterized by $\alpha = 110 \times c/z$ and $\beta = 130 \times c/z$ is depicted in Figure 14. The numerical result has been obtained by using the series expansion of the exponential. The corresponding kernels $\chi(t)$, $N(t)$, $Z(t)$, and $R(t)$ are given in Figure 15.

Figure 14 shows that the propagation kernel can be approximated by the normalized Gaussian (6.2), where

$$t_1(z) = \frac{\alpha}{\beta}\frac{z}{c} \qquad \text{and} \qquad t_2(z) = \sqrt{\frac{2\alpha}{\beta^2}\frac{z}{c}}.$$

Figures 6 and 14 indicate that Gaussian approximation of the propagator kernel is appropriate for relaxation media characterized by large parameters.

8.2 The modified Lorentz medium

The modified Lorentz medium is another absorbing medium for which the normal incidence problem is exactly solvable.

The refraction kernel is given by

$$N(t) = \frac{\omega_p^2}{\nu_0}\sin(\nu_0 t)\exp\left(-\frac{\nu}{2}t\right)H(t), \qquad \nu_0^2 = \omega_0^2 - \frac{\nu^2}{4}.$$

The corresponding susceptibility kernel is

$$\chi(t) = \left(\left(2\frac{\omega_p^2}{\nu_0} + \frac{\omega_p^4}{2\nu_0^3}\right)\sin(\nu_0 t) - \frac{\omega_p^4}{2\nu_0^2}t\cos(\nu_0 t)\right)\exp\left(-\frac{\nu}{2}t\right)H(t).$$

Clearly, the dynamic of the charges in modified Lorentz medium is similar to that in the single-resonance Lorentz medium.

The intrinsic impedance kernel $Z(t)$ is the resolvent kernel of refractive index kernel $N(t)$:

$$Z(t) = -\frac{\omega_p^2}{\sqrt{\nu_0^2+\omega_p^2}}\sin\left(\sqrt{\nu_0^2+\omega_p^2}\,t\right)\exp\left(-\frac{\nu}{2}t\right)H(t).$$

The reflection kernel $-R(t)$ is the resolvent kernel of $Z(t)/2$:

$$R(t) = -\frac{\omega_p^2}{2\sqrt{\nu_0^2+\frac{\omega_p^2}{2}}}\sin\left(\sqrt{\nu_0^2+\frac{\omega_p^2}{2}}\,t\right)\exp\left(-\frac{\nu}{2}t\right)H(t).$$

The operator $\exp(z\mathcal{G}) := 1 + P(z;\cdot)*$ can be factored as $\exp(z\mathcal{G}_0)\,\overline{\exp(z\mathcal{G}_0)}$, where the operator

$$\mathcal{G}_0 = \left(\frac{b\omega_p^2}{2ic\nu_0}\exp(-bt)H(t)\right)*, \qquad b = \nu/2 - i\nu_0,$$

and the bar denotes the complex conjugate. Straightforward computations using series expansion and the identity (6.1) shows that $\exp(z\mathcal{G}_0) = 1 + P_0(z;\cdot)*$ where the kernel

$$P_0(z;t) = -a\frac{J_1\left(2\sqrt{at}\right)}{\sqrt{at}}e^{-bt}H(t) = -a\left(J_0\left(2\sqrt{at}\right) + J_2\left(2\sqrt{at}\right)\right)e^{-bt}H(t)$$

and the complex frequency

$$a(z) = \frac{-b\omega_p^2 z}{2ic\nu_0} = \frac{(\nu_0 + i\nu/2)\omega_p^2 z}{2c\nu_0}.$$

Consequently, the propagator kernel is

$$P(z;t) = P_0(z;t) + \overline{P_0(z;t)} + \Big(P_0(z;\cdot) * \overline{P_0(z;\cdot)}\Big)(t).$$

for the modified Lorentz medium.

The propagation kernel, $P(z;t)$, at fixed propagation depth, z, for the modified Lorentz half-space characterized by $\omega_p = 103\times c/z$, $\omega_0 = 146\times c/z$, and $\nu = 19\times c/z$ is depicted in Figure 16. The parameters have been chosen such that the response matches the response of the Lorentz medium discussed in Section 7, cf Figure 8. The numerical result has been obtained using the integral equation (4.13). The propagator rule (4.19) was used once. The corresponding kernels $\chi(t)$, $N(t)$, $Z(t)$, and $R(t)$ are given in Figures 17–18. Exact solutions and numerical results are compared.

Figure 16 shows that the propagation kernel of the modified Lorentz medium can be approximated by Brillouin's forerunner (6.3) close to the quasilatent time. The quasilatent time, $t_0(z)$, and the scaling times, $t_2(z)$ and $t_3(z)$, are given by

$$t_0(z) = \frac{\omega_p^2}{\omega_0^2}\frac{z}{c} = \frac{z}{2c}, \quad t_2(z) = \sqrt{\frac{2\nu\omega_p^2}{\omega_0^4}\frac{z}{c}}, \quad t_3(z) = \left(\frac{3\omega_p^2(\omega_0^2-\nu^2)}{\omega_0^6}\frac{z}{c}\right)^{\frac{1}{3}}$$

in this case, see Ref. 12. Figure 16 indicates that the numerical method and Brillouin's forerunner overestimate the propagating signal at the first maximum after the quasilatent time.

In the non-absorbing case $\nu = 0$, $a(z) = \omega_p^2 z/(2c)$ is real and $b = -i\omega_0$ is purely imaginary. Defining

$$c(z,t) = -a(z)\left(J_0\left(2\sqrt{a(z)t}\right) + J_2\left(2\sqrt{a(z)t}\right)\right)\cos(\omega_0 t)H(t),$$
$$s(z,t) = -a(z)\left(J_0\left(2\sqrt{a(z)t}\right) + J_2\left(2\sqrt{a(z)t}\right)\right)\sin(\omega_0 t)H(t),$$

the expression for the propagator kernel simplifies to

$$P(z;t) = 2c(z,t) + \big(c(z,\cdot) * c(z,\cdot)\big)(t) + \big(s(z,\cdot) * s(z,\cdot)\big)(t).$$

Letting $\omega_0 \searrow 0$ in the previous expression yields

$$P(z;t) = c(2z,t) = -\frac{\omega_p^2 z}{c}\left(J_0\left(2\omega_p\sqrt{\frac{zt}{c}}\right) + J_2\left(2\omega_p\sqrt{\frac{zt}{c}}\right)\right)H(t). \tag{8.1}$$

This propagator kernel corresponds to the susceptibility kernel

$$\chi(t) = \left(2\omega_p^2 t + \frac{\omega_p^4 t^3}{6}\right)H(t)$$

and the refractive kernel

$$N(t) = \omega_p^2 t H(t).$$

The propagator kernel (8.1), the impedance kernel

$$Z(t) = -\omega_p \sin(\omega_p t) H(t),$$

and the reflection kernel

$$R(t) = -\frac{\omega_p}{\sqrt{2}} \sin\left(\frac{\omega_p}{\sqrt{2}} t\right) H(t)$$

for the case $\omega_p = 10/3 \times z/c$ are depicted in Figure 19. Numerical results, based on the integral equation (4.13), are given for comparison. Notice that this medium is not dissipative, cf equation (2.3).

Conclusion

A number of exact solutions to pulse propagation problems in dispersive dielectrics is given. These are of independent interest. The exact solutions are compared to numerical results obtained by a time-domain propagator method based on a scalar, causal fundamental solution of the one-dimensional dispersive wave operator. The results also indicate that the numerical method is very efficient provided that the propagation distance is not too large. The results indicate that the time-domain theory for forerunners is applicable at (comparatively) large propagation depths.

Acknowledgment

The work reported in this paper is supported by a grant from the Swedish Research Council for Engineering Sciences, and its support is gratefully acknowledged.

Appendix A Resolvent operators and kernels

The resolvent operator or the inverse operator of the relative permittivity operator (2.2) is an integral operator on the form

$$\mathcal{E}_r^{-1} \equiv (1 + \chi_{\text{res}}*) = (\delta + \chi_{\text{res}}) * .$$

This operator satisfies the equation $\mathcal{E}_r^{-1}\mathcal{E}_r = \mathcal{E}_r\mathcal{E}_r^{-1} = 1$.

The resolvent kernel of $\chi(t)$ is denoted by $\chi_{\text{res}}(t)$ and satisfies the linear Volterra integral equation of the second kind

$$\chi_{\text{res}}(t) + \chi(t) + (\chi_{\text{res}} * \chi)(t) = 0.$$

This equation has a unique solution in the space of bounded and smooth functions in each bounded time-interval $0 < t < T$. Explicitly, the resolvent kernel can be represented by the function series

$$\chi_{\rm res}(t) = \sum_{k=1}^{\infty}(-1)^k \left((\chi*)^{k-1}\chi\right)(t).$$

The resolvent kernel vanishes for $t < 0$ and has a finite jump-discontinuity at $t = 0$ if and only if $\chi(t)$ has such a discontinuity: $\chi_{\rm res}(+0) = -\chi(+0)$.

The resolvent kernel of the susceptibility kernel of the Debye model is

$$\chi_{\rm res}(t) = -\alpha \exp\left(-(\alpha+\beta)t\right)H(t),$$

and the corresponding result for the Lorentz medium is

$$\chi_{\rm res}(t) = -\frac{\omega_p^2}{\omega}\sin(\omega t)\exp\left(-\frac{\nu}{2}t\right)H(t),$$

where the frequency ω is given by equation (3.6). In other words, the resolvent kernel of a Debye kernel is a Debye kernel and the resolvent kernel of a Lorentz kernel is a Lorentz kernel. For the Debye-Lorentz medium, the resolvent kernel of the susceptibility kernel is

$$\chi_{\rm res}(t) = -\omega_p \sin(\omega_p t)\exp(-\omega_0 t)H(t).$$

These results are easily obtained by Laplace transform technique.

Results for two more complicated dispersive materials are now presented. The resolvent kernel of the double-Debye kernel (3.7) is another double-Debye kernel:

$$\chi_{\rm res}(t) = -\alpha^+ \exp(-\beta^+ t)H(t) - \alpha^- \exp(-\beta^- t)H(t), \tag{A.1}$$

where

$$\begin{aligned} 2\beta^{\pm} &= \alpha_1+\beta_1+\alpha_2+\beta_2 \pm \sqrt{(\alpha_1-\beta_1+\alpha_2+\beta_2)^2 + 4\alpha_1(\beta_1-\beta_2)}, \\ \alpha^{\pm} &= \frac{\beta_1-\beta_2}{\frac{(\beta^{\mp}-\beta_2)}{(\beta^{\pm}-\beta_2)} - \frac{(\beta^{\mp}-\beta_1)}{(\beta^{\pm}-\beta_1)}}. \end{aligned}$$

Notice that $0 \le \beta_2 < \beta^- < \beta_1 < \beta^+$ and that $\alpha^{\pm} \ge 0$. This result is easily obtained by observing that causal convolution of two exponentials is a linear combination of the exponentials involved. The resolvent kernel of the double-Debye kernel may be relevant for Maxwell Garnett mixing of two dispersive Debye materials and for modelling fog.

The resolvent kernel of the double-Lorentz kernel (3.8) for which $\nu_1 = \nu_2 = \nu$ and $\nu_{02} < \nu_{01}$ is another double-Lorentz kernel:

$$\chi_{\rm res}(t) = -\left(\frac{\omega_{p+}^2}{\nu_{0+}}\sin(\nu_{0+}t) + \frac{\omega_{p-}^2}{\nu_{0-}}\sin(\nu_{0-}t)\right)\exp\left(-\frac{\nu}{2}t\right)H(t), \tag{A.2}$$

where

$$\begin{aligned}\nu_{0\pm} &= \sqrt{\frac{\nu_{01}^2+\nu_{02}^2+\omega_{p1}^2+\omega_{p2}^2 \pm \sqrt{\left(-\nu_{01}^2+\nu_{02}^2+\omega_{p1}^2+\omega_{p2}^2\right)^2+4\omega_{p1}^2(\nu_{01}^2-\nu_{02}^2)}}{2}},\\ \omega_{p\pm} &= \sqrt{\frac{\pm(\nu_{0\mp}^2-\nu_{02}^2)^{-1}\mp(\nu_{0\mp}^2-\nu_{01}^2)^{-1}}{(\nu_{0+}^2-\nu_{01}^2)^{-1}(\nu_{0-}^2-\nu_{02}^2)^{-1}+(\nu_{0+}^2-\nu_{02}^2)^{-1}(\nu_{01}^2-\nu_{0-}^2)^{-1}}}.\end{aligned}$$

Notice that $0 \leq \nu_{02} < \nu_{0-} < \nu_{01} < \nu_{0+}$ and $\omega_{p-} \geq 0$. The result follows from the observation that causal convolution of two sinusoidals is a linear combination of the sinusoidals involved. If the general case ($\nu_{02} \neq \nu_{01}$), the resolvent kernel of the double-Lorentz kernel is no longer a double-Lorentz kernel.

Appendix B Special functions for Lorentz media

For brevity, the functions $A_f(t)$, $a_f(t)$, $C_f(t)$, $c_f(t)$, where f denotes an arbitrary frequency, are introduced. These functions are

$$A_f(t) = J_0(ft) \tag{B.1}$$

with time derivative

$$a_f(t) = \frac{dA_f(t)}{dt} = -fJ_1(ft) \tag{B.2}$$

and

$$C_f(t) = \frac{f}{t}J_1(ft) = \frac{f^2}{2}\big(J_0(ft) + J_2(ft)\big) \tag{B.3}$$

with time derivative

$$c_f(t) = \frac{dC_f(t)}{dt} = -\frac{f^2}{t}J_2(ft) = -\frac{f^3}{4}\big(J_1(ft) + J_3(ft)\big). \tag{B.4}$$

The functions $J_n(x)$ are Bessel functions of the first kind.

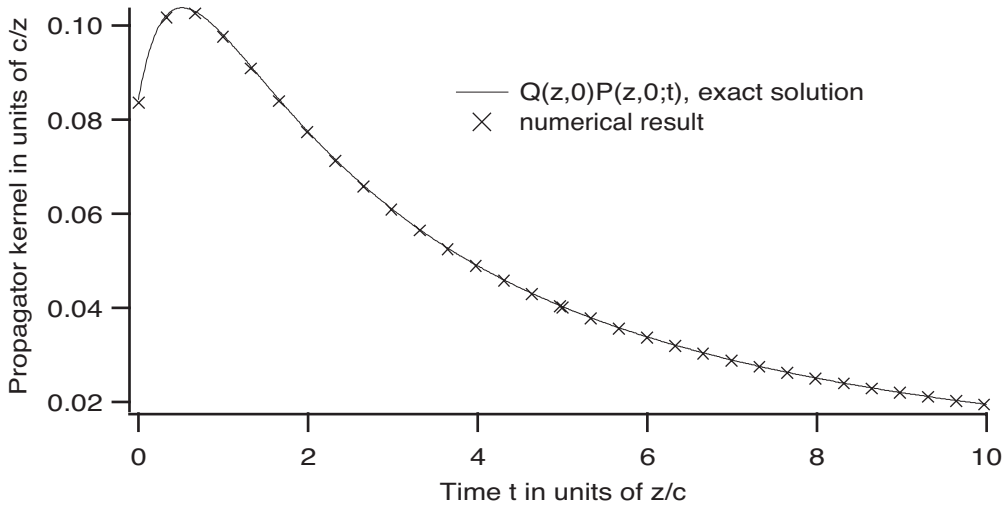

Figure 2: The propagator kernel $Q(z)P(z;t)$ for a non-absorbing Debye half-space characterized by $\alpha = 10 \times c/z = \sigma/(c\eta)$. 64 data points were used at the equidistant discretization of the time interval $0 < t < 2 \times z/c$.

References

[1] M. Abramowitz and I.A. Stegun, editors. *Handbook of Mathematical Functions.* Applied Mathematics Series No. 55. National Bureau of Standards, Washington D.C., 1970.

[2] R.S. Beezley and R.J. Krueger. An electromagnetic inverse problem for dispersive media. *J. Math. Phys.*, **26**(2), 317–325, 1985.

[3] L. Brillouin. Über die Fortpflanzung des Lichtes in dispergierenden Medien. *Ann. Phys.*, **44**, 203–240, 1914.

[4] L. Brillouin. *Wave propagation and group velocity.* Academic Press, New York, 1960.

[5] A. Chelkowski. *Dielectric Physics.* Elsevier, Amsterdam, 1980.

[6] S.L. Dvorak and D.G. Dudly. Propagation of Ultra-Wide-Band Electromagnetic Pulses Trough Dispersive Media. *IEEE Trans. Electromagn. Compatibility*, **37**(2), 192–200, 1995.

[7] L.B. Felsen and N. Marcuvitz. *Radiation and scattering of waves.* Prentice-Hall, Inc., Englewood Cliffs, New Jersey, first edition, 1973.

[8] L. Hörmander. *The Analysis of Linear Partial Differential Operators I.* Grundlehren der matematischen Wissenshaften 256. Springer, Berlin Heidelberg, 1983.

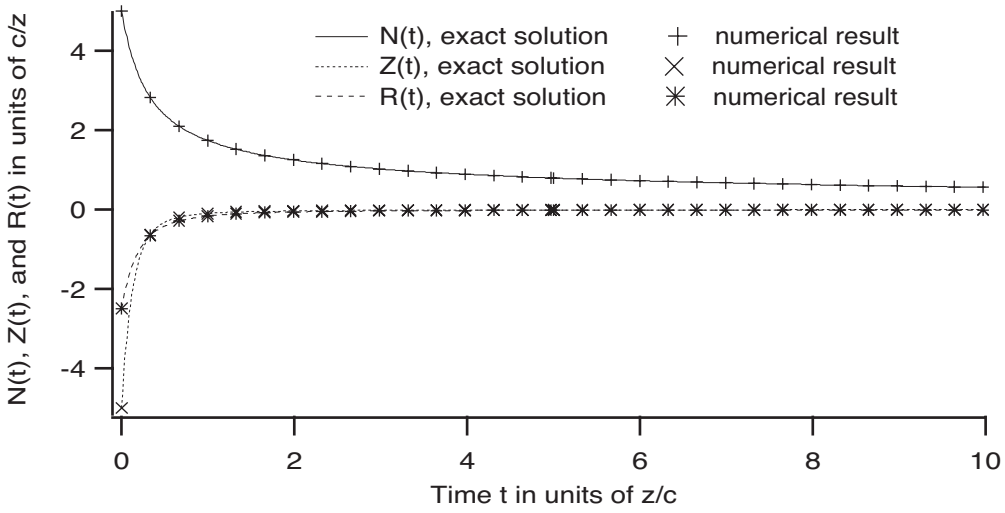

Figure 3: The kernels $N(t)$, $Z(t)$, and $R(t)$ for a non-absorbing Debye half-space characterized by $\alpha = 10 \times c/z$. 64 data points were used at the equidistant discretization of the time interval $0 < t < 2 \times z/c$.

[9] J.D. Jackson. *Classical Electrodynamics*. John Wiley & Sons, New York, second edition, 1975.

[10] A. Karlsson. Wave propagators for transient waves in one-dimensional media. *Wave Motion*, **24**(1), 85–99, 1996.

[11] A. Karlsson and G. Kristensson. Constitutive relations, dissipation and reciprocity for the Maxwell equations in the time domain. *J. Electro. Waves Applic.*, **6**(5/6), 537–551, 1992.

[12] A. Karlsson and S. Rikte. The time-domain theory of forerunners. Technical Report LUTEDX/(TEAT-7054)/1–31/(1997), Lund Institute of Technology, Department of Electromagnetic Theory, P.O. Box 118, S-211 00 Lund, Sweden, 1996.

[13] G. Kristensson. Direct and inverse scattering problems in dispersive media—Green's functions and invariant imbedding techniques. In R. Kleinman, R. Kress, and E. Martensen, editors, *Direct and Inverse Boundary Value Problems*, Methoden und Verfahren der Mathematischen Physik, Band 37, pages 105–119, Frankfurt am Main, 1991. Peter Lang.

[14] G. Kristensson. Transient electromagnetic wave propagation in waveguides. *J. Electro. Waves Applic.*, **9**(5/6), 645–671, 1995.

[15] H.J. Liebe, T. Manabe, and G.A. Hufford. Millimeter-wave attenuation and delay rates due to fog/cloud conditions. *IEEE Transactions on Antennas and Propagation*, **37**(12), 1617–1623, December 1989.

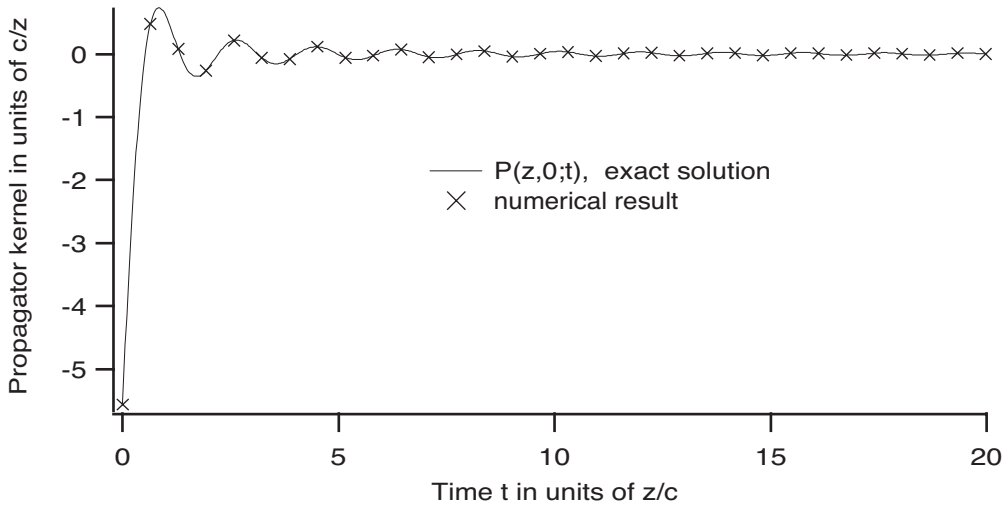

Figure 4: The propagator kernel $P(z;t)$ for a non-absorbing Debye-Lorentz half-space characterized by $\omega_p = 10/3 \times c/z$. 64 data points were used at the equidistant discretization of the time interval $0 < t < 2 \times z/c$.

[16] K.E. Oughstun and G.C. Sherman. Propagation of electromagnetic pulses in a linear dispersive medium with absorption (the Lorentz medium). *J. Opt. Soc. Am. B*, **5**(4), 817–849, 1988.

[17] K.E. Oughstun and G.C. Sherman. *Electromagnetic Pulse Propagation in Causal Dielectrics*. Springer-Verlag, Berlin Heidelberg, 1994.

[18] E.J. Post. *Formal Structure of Electromagnetics*. North-Holland, Amsterdam, 1962.

[19] T.M. Roberts. Causality theorems. In J.P. Corones, G. Kristensson, P. Nelson, and D.L. Seth, editors, *Invariant Imbedding and Inverse Problems*. SIAM, 1992.

[20] A. Sommerfeld. Über die Fortpflanzung des Lichtes in dispergierenden Medien. *Ann. Phys.*, **44**, 177–202, 1914.

[21] J.A. Stratton. *Electromagnetic Theory*. McGraw-Hill, New York, N.Y., 1941.

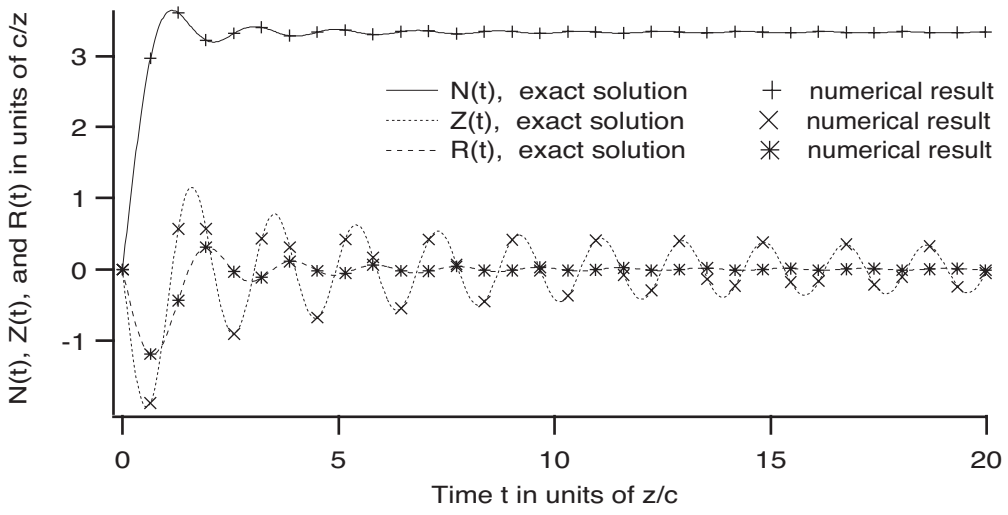

Figure 5: The kernels $N(t)$, $Z(t)$, and $R(t)$ for a non-absorbing Debye-Lorentz half-space characterized by $\omega_p = 10/3 \times c/z$. 64 data points were used at the equidistant discretization of the time interval $0 < t < 2 \times z/c$.

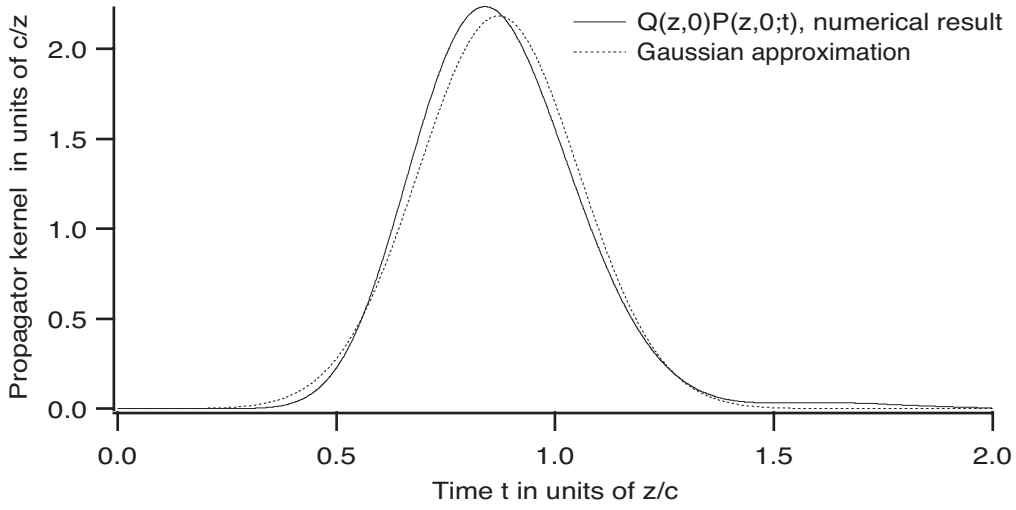

Figure 6: The propagator kernel $Q(z)P(z;t)$ for a Debye half-space characterized by $\alpha = 100 \times c/z$ and $\beta = 40 \times c/z$. 4096 data points were used at the equidistant discretization of the time interval $0 < t < 2 \times z/c$.

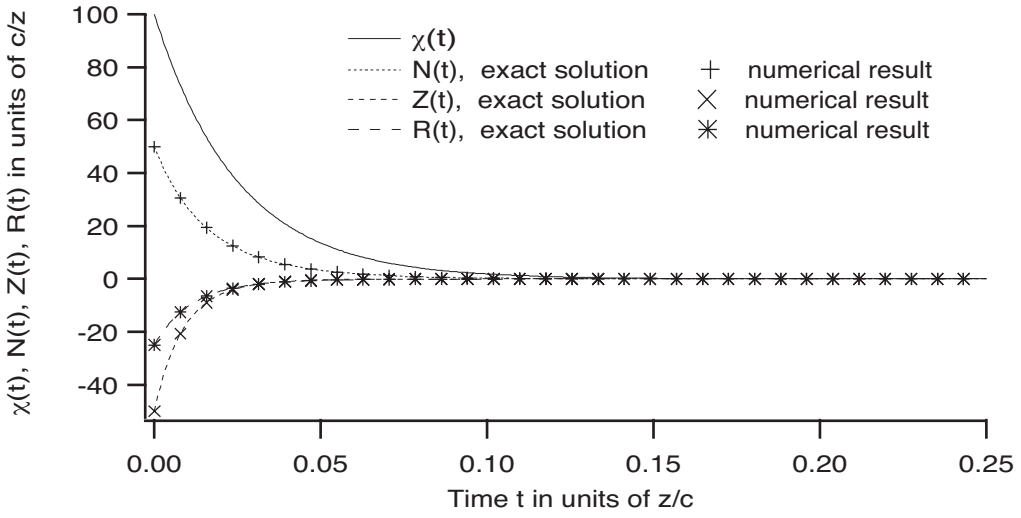

Figure 7: The kernels $\chi(t)$, $N(t)$, $Z(t)$, and $R(t)$ for a Debye half-space characterized by $\alpha = 100 \times c/z$ and $\beta = 40 \times c/z$. 4096 data points were used at the equidistant discretization of the time interval $0 < t < 2 \times z/c$.

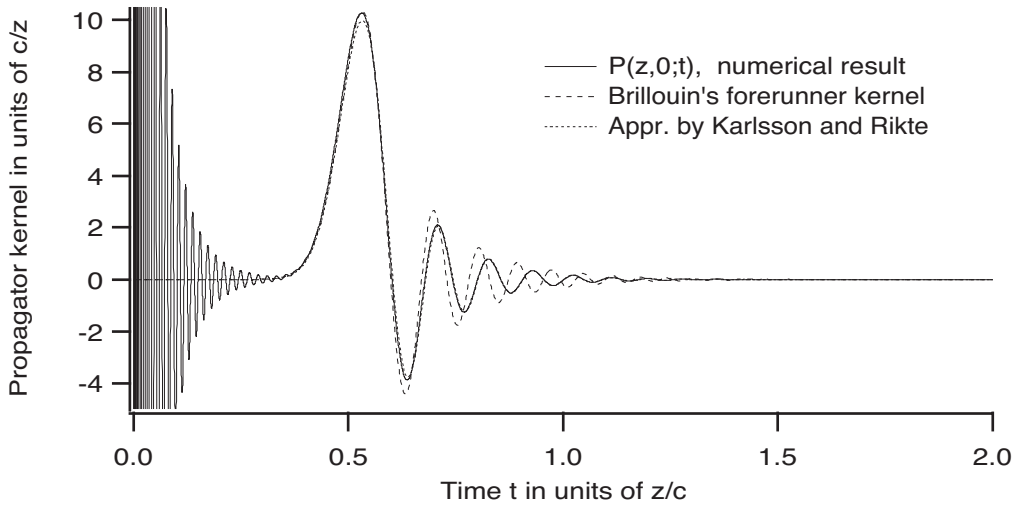

Figure 8: The propagator kernel $P(z;t)$ for a single-resonance Lorentz half-space characterized by Brillouin's parameters. 32768 data points were used at the equidistant discretization of the time interval $0 < t < 2 \times z/c$. The propagator rule was used once at the computation.

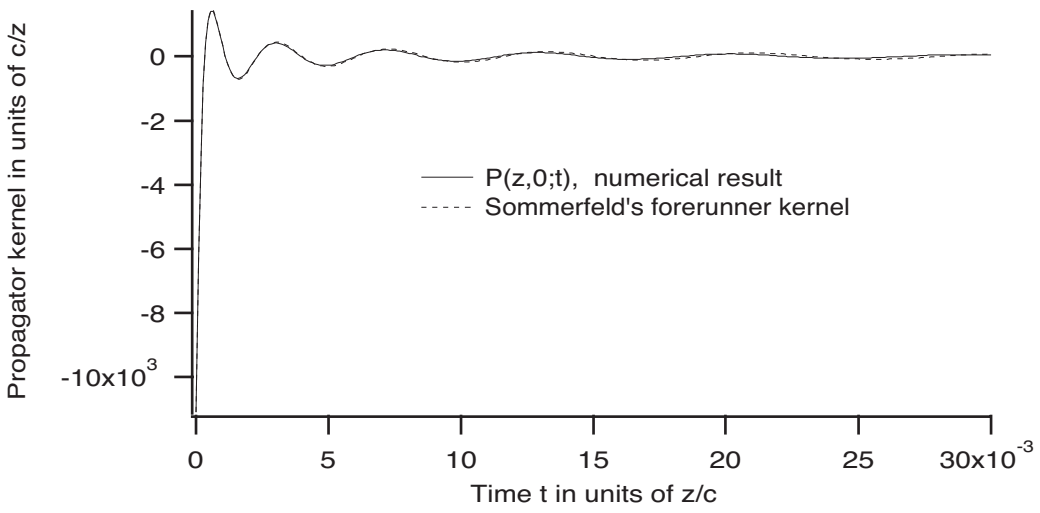

Figure 9: The propagator kernel $P(z;t)$ for a single-resonance Lorentz half-space characterized by Brillouin's parameters.

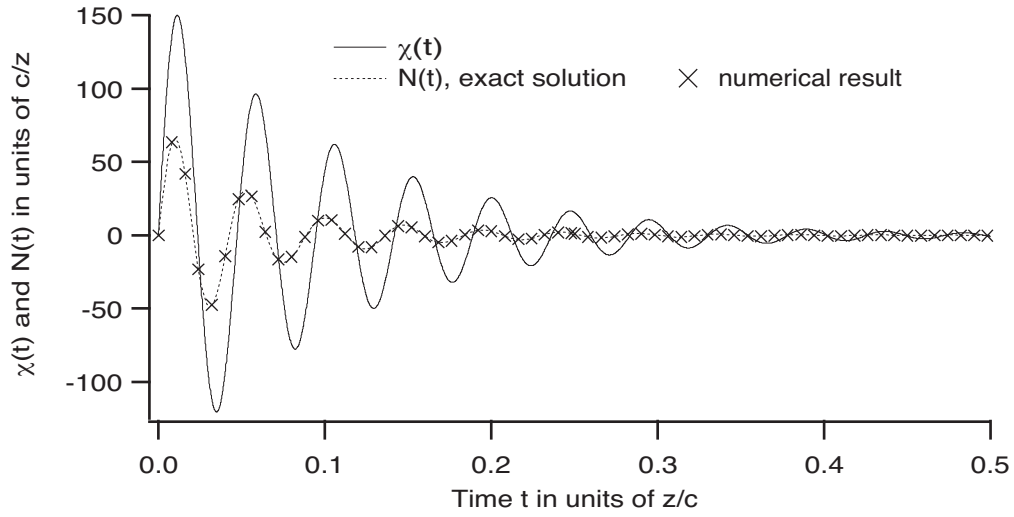

Figure 10: The kernels $\chi(t)$ and $N(t)$ for a single-resonance Lorentz half-space characterized by Brillouin's parameters. 1024 data points were used at the equidistant discretization of the time interval $0 < t < 2 \times z/c$.

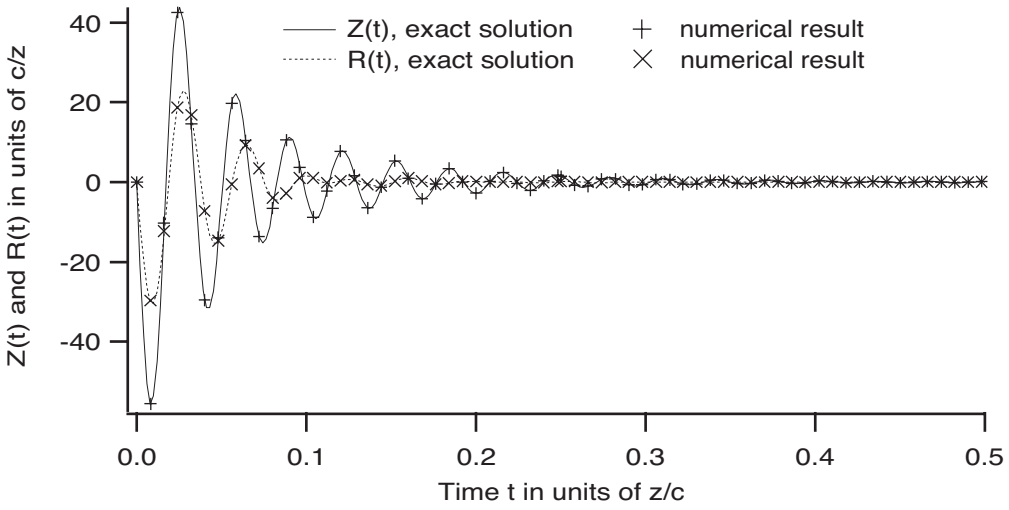

Figure 11: The kernels $Z(t)$ and $R(t)$ for a single-resonance Lorentz half-space characterized by Brillouin's parameters. 1024 data points were used at the equidistant discretization of the time interval $0 < t < 2 \times z/c$.

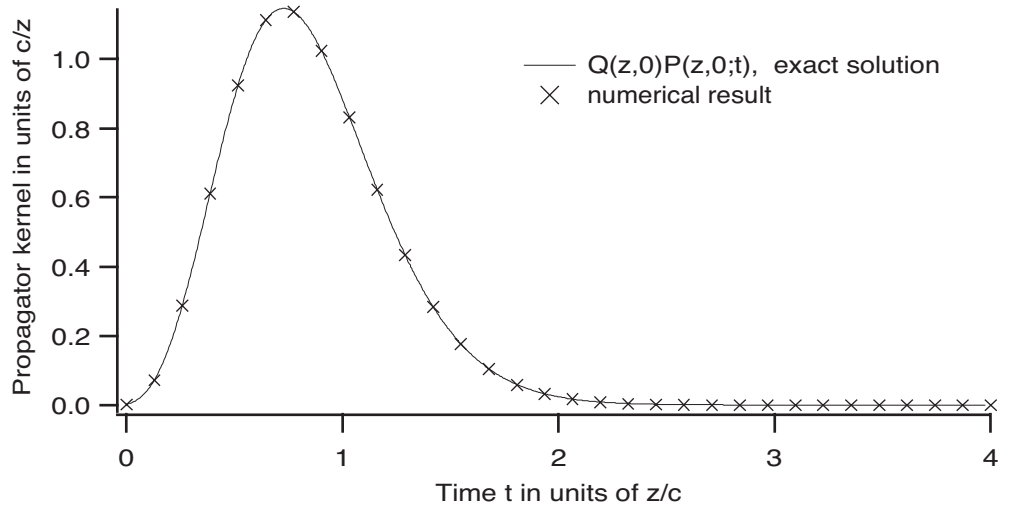

Figure 12: The propagator kernel $Q(z)P(z;t)$ for a modified Debye half-space characterized by $\alpha = 11 \times c/z$ and $\beta = 13 \times c/z$. 512 data points were used at the equidistant discretization of the time interval $0 < t < 2 \times z/c$.

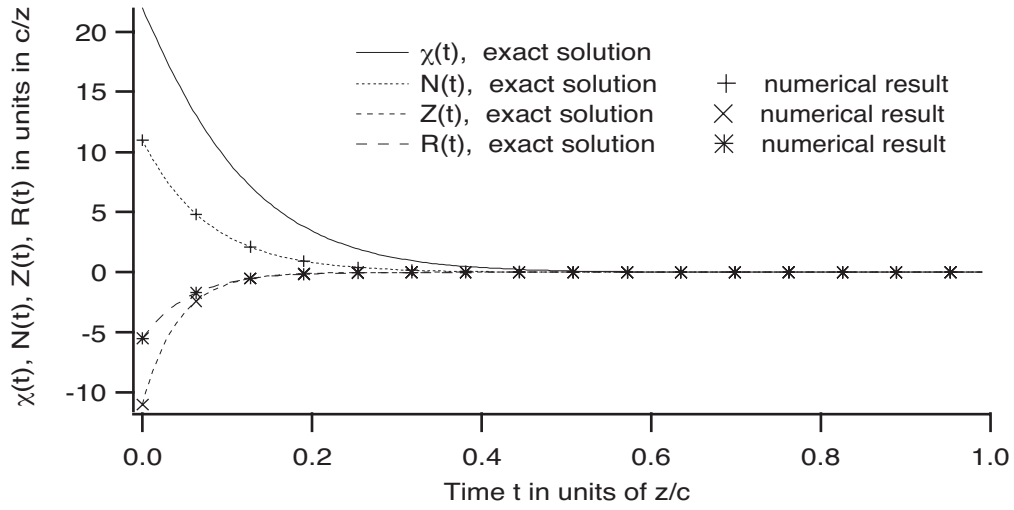

Figure 13: The kernels $\chi(t)$, $N(t)$, $Z(t)$, and $R(t)$ for a modified Debye half-space characterized by $\alpha = 11 \times c/z$ and $\beta = 13 \times c/z$. 512 data points were used at the equidistant discretization of the time interval $0 < t < 2 \times z/c$.

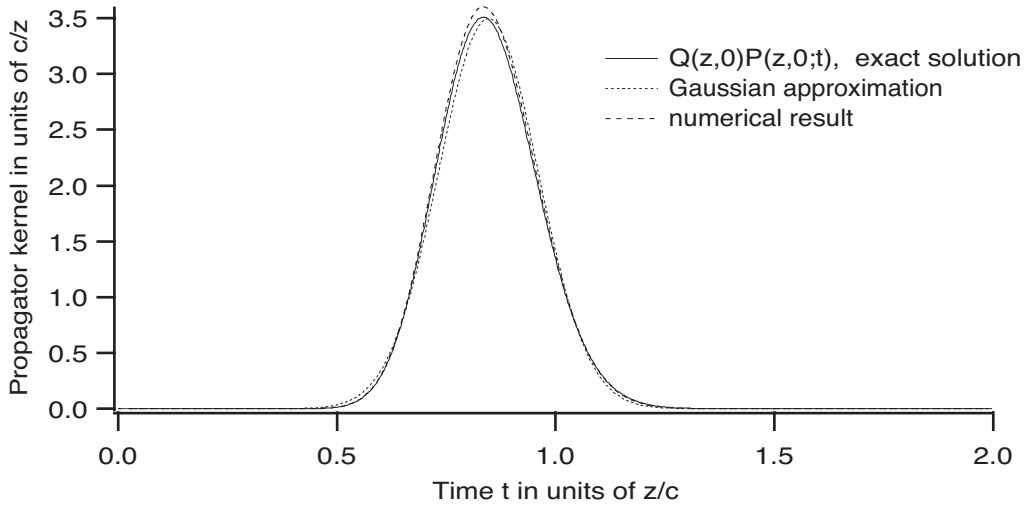

Figure 14: The propagator kernel $Q(z)P(z;t)$ for a modified Debye half-space characterized by $\alpha = 110 \times c/z$ and $\beta = 130 \times c/z$. 8192 data points are used at the equidistant discretization of the time interval $0 < t < 2 \times z/c$.

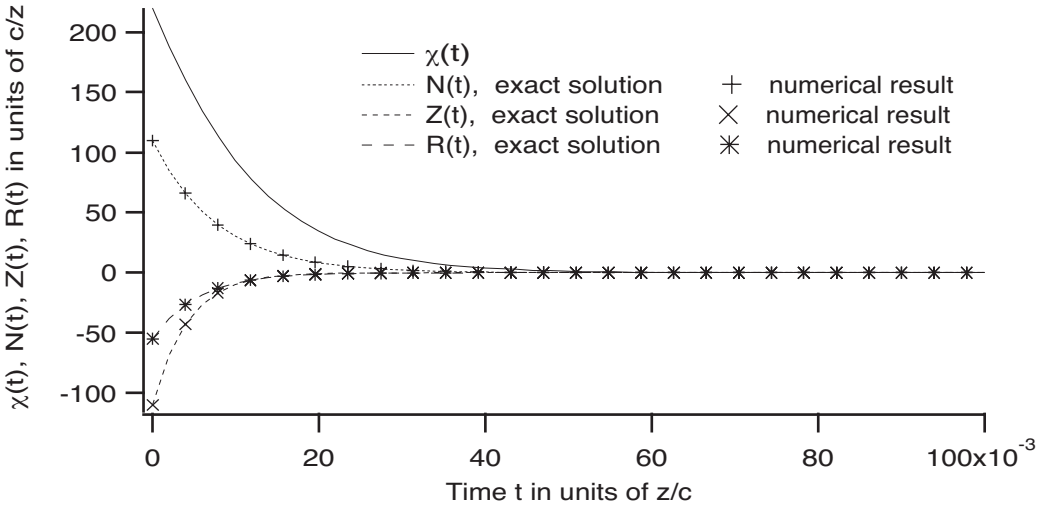

Figure 15: The kernels $\chi(t)$, $N(t)$, $Z(t)$, and $R(t)$ for a modified Debye half-space characterized by $\alpha = 110 \times c/z$ and $\beta = 130 \times c/z$. 4096 data points were used at the equidistant discretization of the time interval $0 < t < 2 \times z/c$.

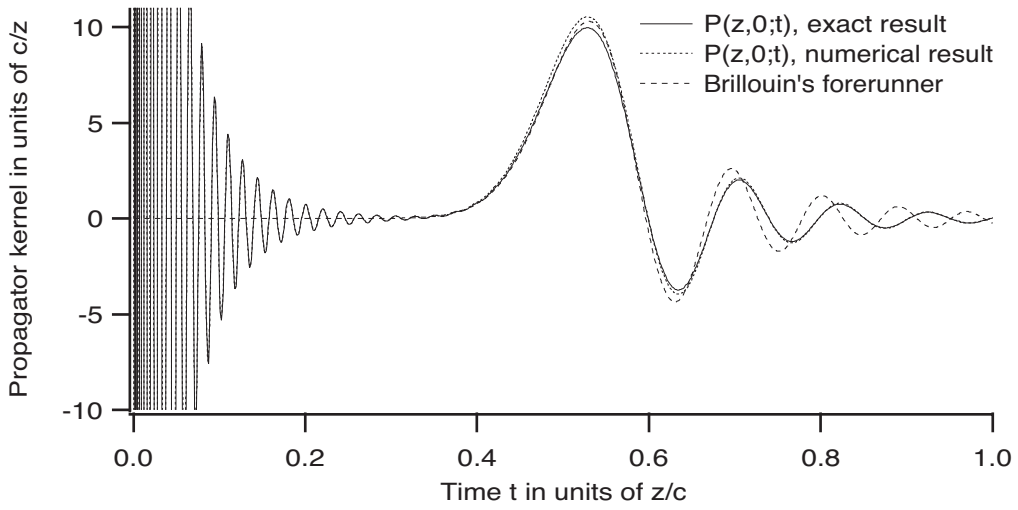

Figure 16: The propagator kernel $P(z;t)$ for a modified Lorentz half-space characterized by $\omega_p = 103 \times c/z$, $\omega_0 = 146 \times c/z$ and $\nu = 19 \times c/z$. 16768 data points were used at the equidistant discretization of the time interval $0 < t < z/c$. The propagator rule was used once at the calculation.

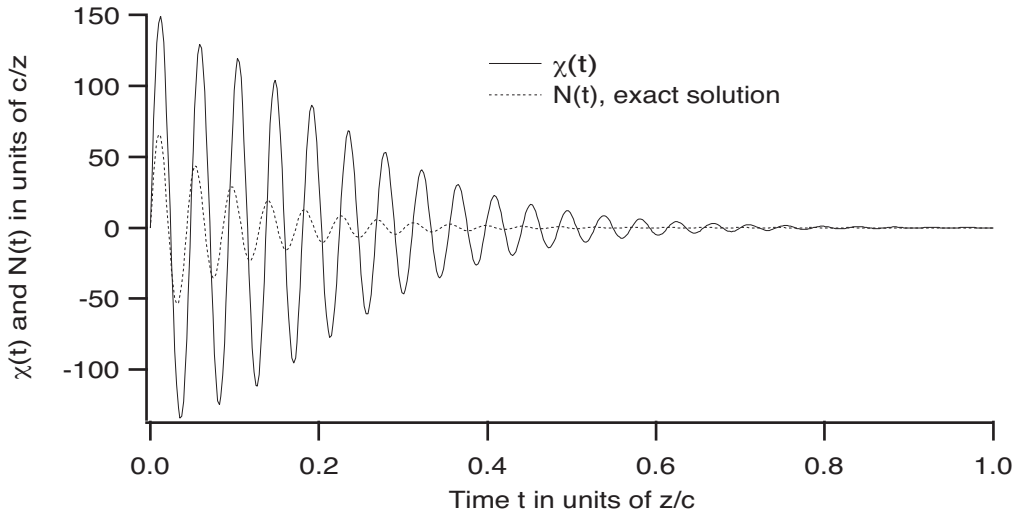

Figure 17: The kernels $\chi(t)$ and $N(t)$ for a modified Lorentz half-space characterized by $\omega_p = 103 \times c/z$, $\omega_0 = 146 \times c/z$ and $\nu = 19 \times c/z$.

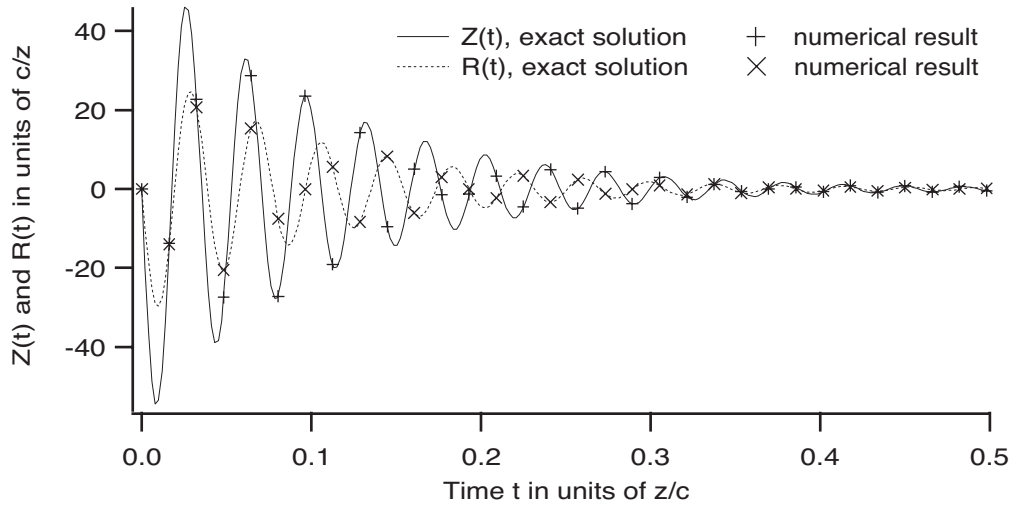

Figure 18: The kernels $Z(t)$ and $R(t)$ for a modified Lorentz half-space characterized by $\omega_p = 103 \times c/z$, $\omega_0 = 146 \times c/z$ and $\nu = 19 \times c/z$. 512 data points were used at the equidistant discretization of the time interval $0 < t < z/c$.

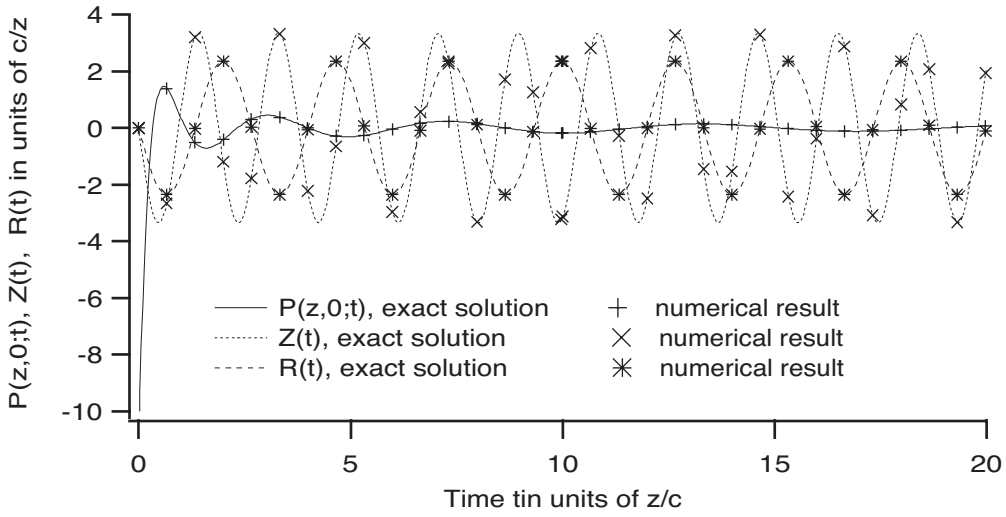

Figure 19: The kernels $P(z;t)$, $Z(t)$, and $R(t)$ for a non-absorbing modified Lorentz half-space characterized by $\omega_p = 10/3 \times c/z$. 64 data points were used at the equidistant discretization of the time interval $0 < t < 2 \times z/c$.